Geochemistry, Geophysics, Geosystems®

RESEARCH ARTICLE
10.1029/2024GC011470

Combustion Completeness and Sample Location Determine Wildfire Ash Leachate Chemistry

Micheline Campbell[1], Pauline C. Treble[1,2], Liza K. McDonough[2], Sebastian Naeher[3], Andy Baker[1,2], Pauline F. Grierson[4], Henri Wong[2], and Martin S. Andersen[5]

[1]School of Biological, Earth, and Environmental Sciences, UNSW Sydney, Sydney, NSW, Australia, [2]ANSTO, Lucas Heights, NSW, Australia, [3]GNS Science, Lower Hutt, New Zealand, [4]School of Biological Sciences, The University of Western Australia, Perth, WA, Australia, [5]Water Research Laboratory, School of Civil and Environmental Engineering, UNSW Sydney, Sydney, NSW, Australia

Key Points:

- Stalagmites record past fire activity through changes in inorganic and organic chemistry sourced from ashes
- Wildfire ash leachate chemistry will aid interpretation of proxy fire data
- Results show that inorganic chemistry varies with burn severity and sample location, and the pyrogenic biomarker signal is less clear

Supporting Information:

Supporting Information may be found in the online version of this article.

Correspondence to:

M. Campbell,
micheline.campbell@unsw.edu.au

Citation:

Campbell, M., Treble, P. C., McDonough, L. K., Naeher, S., Baker, A., Grierson, P. F., et al. (2024). Combustion completeness and sample location determine wildfire ash leachate chemistry. *Geochemistry, Geophysics, Geosystems*, *25*, e2024GC011470. https://doi.org/10.1029/2024GC011470

Received 23 JAN 2024
Accepted 18 APR 2024

Author Contributions:

Conceptualization: Micheline Campbell, Pauline C. Treble, Liza K. McDonough, Andy Baker
Data curation: Micheline Campbell, Liza K. McDonough, Sebastian Naeher, Henri Wong
Formal analysis: Micheline Campbell
Funding acquisition: Pauline C. Treble, Andy Baker
Investigation: Micheline Campbell, Pauline C. Treble, Liza K. McDonough, Sebastian Naeher, Andy Baker, Pauline F. Grierson, Henri Wong
Methodology: Micheline Campbell, Sebastian Naeher, Henri Wong

Abstract Understanding past fire regimes and how they vary with climate, human activity, and vegetation patterns is fundamental to the mitigation and management of changing fire regimes as anthropogenic climate change progresses. Ash-derived trace elements and pyrogenic biomarkers from speleothems have recently been shown to record past fire activity in speleothems from both Australia and North America. This calls for an empirical study of ash geochemistry to aid the interpretation of speleothem palaeofire proxy records. Here we present analyses of leached ashes collected following fires in southwest and southeast Australia. We include a suite of inorganic elemental data from the water-soluble fraction of ash as well as a selection of organic analytes (pyrogenic lipid biomarkers). We also present elemental data from leachates of soils collected from sites in southwest Australia. We demonstrate that the water-soluble fraction of ash differs from the water-soluble fraction of soils, with trace and minor element concentrations in ash leachates varying with combustion completeness (burn severity) and sample location. Changes in some lipid biomarker concentrations extracted from ashes may reflect burn severity. Our results contribute to building a process-based understanding of how speleothem geochemistry may record fire frequency and severity, and suggest that more research is needed to understand the transport pathways for the inclusion of pyrogenic biomarkers in speleothems. Our results also demonstrate that potential contaminant loads from ashes are much higher than from soils, with implications for the management of karst catchments, which are a critical water resource.

Plain Language Summary Understanding past fire activity is necessary to develop effective land management strategies to manage activity. Recently, stalagmites (naturally forming cave decorations) have been shown to record past fire information through chemical changes. The chemical changes are due to post-fire leaching of wildfire ash. By investigating wildfire ash chemistry, we will be able to improve our interpretations of the stalagmite past fire signal. Our results show that ash chemistry from Australian fires varies with burn severity and sample location, and that the ash chemistry and soil chemistry differ. Results suggest that stalagmites may record burn severity as well as fire frequency. We also suggest that the potential impact of high concentrations of potential contaminants in wildfire ash on karst aquifers should be further investigated.

1. Introduction

Wildfires occur on all ice-free continents, affecting about 40% of the terrestrial biome (Chapin et al., 2011). Each year, an estimated ~300–460 million ha burn globally (Giglio et al., 2006; Lizundia-Loiola et al., 2020; Wei et al., 2021). Globally, there has been an observed increase in fire weather, which has contributed to an increase in burned area in some regions (noting that fire occurrence is modulated by more than just dangerous fire weather) (Jones et al., 2022). Observational records are too short to fully understand fire regimes, so proxy palaeofire data are sourced from natural archives such as sediment cores, ice cores, and tree scars. These proxy archives have allowed past fire activity to be reconstructed at local (e.g., Rehn et al., 2021), continental (e.g., Zennaro et al., 2015), and global scales (e.g., Marlon et al., 2008). In recent years, speleothems (primarily stalagmites) have been developed as archives of past fire activity, with both inorganic proxies (predominantly trace metals) and pyrogenic biomarkers used to investigate past fire activity (Argiriadis et al., 2019, 2023; M. Campbell et al., 2023; Homann et al., 2022, 2023; McDonough et al., 2022). The inorganic fire proxy signal in speleothems is thought to be sourced from ashes deposited over the cave, which are subsequently leached by rainfall, transported via karst flowpaths, and deposited with speleothem calcite. It is less clear whether the pyrogenic biomarker

Project administration: Pauline C. Treble, Liza K. McDonough, Andy Baker
Resources: Pauline C. Treble, Andy Baker
Supervision: Pauline C. Treble, Andy Baker
Validation: Sebastian Naeher, Henri Wong, Martin S. Andersen
Visualization: Micheline Campbell
Writing – original draft: Micheline Campbell, Pauline C. Treble, Sebastian Naeher, Pauline F. Grierson
Writing – review & editing: Micheline Campbell, Pauline C. Treble, Liza K. McDonough, Sebastian Naeher, Andy Baker, Pauline F. Grierson, Henri Wong, Martin S. Andersen

signal is transported via the leaching of ashes or via aerosol inputs (Homann et al., 2023), although Homann et al. (2022) sampled cave dripwaters and demonstrated in that cave that levoglucosan was transported with infiltrating waters through the karst. In any case, refining the interpretation of speleothem palaeofire proxies calls for an empirical study of the geochemistry of ash to inform the interpretation of both organic and inorganic speleothem fire proxy records.

Ash from combusted biomass is generally comprised of charred organic components and minerals. At lower temperatures (usually <450°C), ash is mostly comprised of organic carbon, while at higher temperatures (>450°C), ash is comprised mostly of minerals as inorganic carbonates, and at very high temperatures (>580°C), most remaining minerals are present as oxides (Bodí et al., 2014; Certini, 2005). Ash color is generally related to combustion completeness, with dark, organic-rich ashes formed at lower degrees of combustion, and lighter mineral-rich ashes formed due to greater combustion completeness (Bodí et al., 2014; Roy et al., 2010; Stronach & McNaughton, 1989). White ash is usually more alkaline than black ash due to the solubilization of major elements in ash (Bodí et al., 2014; Pereira et al., 2012; Ulery et al., 1993), with ash pH generally ranging from 9.0 to 13.5 (Khanna et al., 1994; Misra et al., 1993; Yusiharni & Gilkes, 2012). Ash is an expected source of certain elements owing to its sequestration within plant biomass, both living and dead. Calcium, Mg, K, Si, P, Na, S, Al, Fe, Mn, Zn, and associated carbonates (e.g., $CaCO_3$, $MgCO_3$, and K_2CO_3) are normally the dominant inorganic constituents of ash (Bodí et al., 2014; Gabet & Bookter, 2011; Pereira & Úbeda, 2010; Qian et al., 2009). However, their relative amounts and proportions of different elements vary considerably as different elements are volatilized to a lesser or greater extent depending on the temperature of combustion (Bodí et al., 2014; Hogue & Inglett, 2012). Concentrations of elements in ash also reflect differences in sources, that is, which tissues (leaf or wood) have been combusted, as well as variation among species (e.g., Yusiharni & Gilkes, 2012). Sánchez-García et al. (2023) reported that the large variance in their global wildfire ash concentration data set was due to the ecosystem, burn severity, land use history (resulting in legacy contamination) and in situ leaching by rainfall prior to sample collection. In experimental settings, hotter combustion temperatures have been shown to result in Ca/Mg ratios in ash leachates of <1 (Marion et al., 1991; Úbeda et al., 2009). However, in ashes from both experimental studies and wildfires with known burn temperature or severity (Balfour & Woods, 2013; Miotliński et al., 2023; Pereira et al., 2012; Sánchez-García et al., 2023; Santín et al., 2015; Úbeda et al., 2009), the response of both Ca and Mg to burn severity is variable, and none of the published concentrations support the hypothesis that this ratio indicates burn severity.

The legacies of fire impacts on ash and soil are also evident in organic compounds resulting from the combustion of plant material. Pyrogenic biomarkers such as levoglucosan and polycyclic aromatic hydrocarbons (PAHs) are used to investigate past fire activity in environmental archives such as ice and sediment cores, and speleothems (Argiriadis et al., 2019, 2023; Denis et al., 2012; Homann et al., 2022, 2023; Rubino et al., 2016; Vachula et al., 2019). Levoglucosan (1,6-anhydro-β-d-glucopyranose) is a water-soluble anhydrosugar which is formed through the thermal breakdown of cellulose and hemicellulose (Bhattarai et al., 2019; Elias et al., 2001; Li et al., 2021; Simoneit et al., 1999). Levoglucosan is source specific, and unlike other pyrogenic biomarkers, it is not produced by the combustion of fossil fuels, making it a reliable tracer of biomass burning (Elias et al., 2001). While normally associated with particulate matter and smoke, levoglucosan has been shown to be present in black char (Kuo et al., 2008; Otto et al., 2006). Levoglucosan yield from black char has been shown to vary with temperature and plant species (Kuo et al., 2008). Levoglucosan is semi-volatile and can be transported with smoke in the atmosphere, where it has an atmospheric life of ∼26 days (Bai et al., 2013). PAHs are organic molecules characterized by two or more aromatic rings which form by incomplete combustion of biomass and fossil fuels. In the modern era, anthropogenic inputs (e.g., fossil fuels) are the dominant source, and in sediment cores the most recent deposits can be greatly enriched relative to pre-industrial levels (Perrette et al., 2008; Wakeham et al., 1980). The amount and type of PAHs formed by fire are controlled by the maximum temperature, duration, and oxygen level (Blumenstock et al., 2000; Johansson and van Bavel, 2003). At temperatures up to 400°C, low molecular weight PAHs (<252 g/mol; 4-ring compounds) are more abundant in post-fire soils than high molecular weight PAHs (>252 g/mol; 5-ring compounds) (Kim et al., 2011; Rey-Salgueiro et al., 2018; Simon et al., 2016). Karp et al. (2020) describe a temperature optimum for PAH formation between 400 and 600°C. While PAHs adsorb onto organic matter, which limits degradation and bioavailability, levels in post-fire soils have been shown to decline to pre-fire concentrations over time as leaching and erosion mobilizes PAHs (Kim et al., 2011; Simon et al., 2016; Yang et al., 2010). Some research has attributed high soil PAH levels to ash

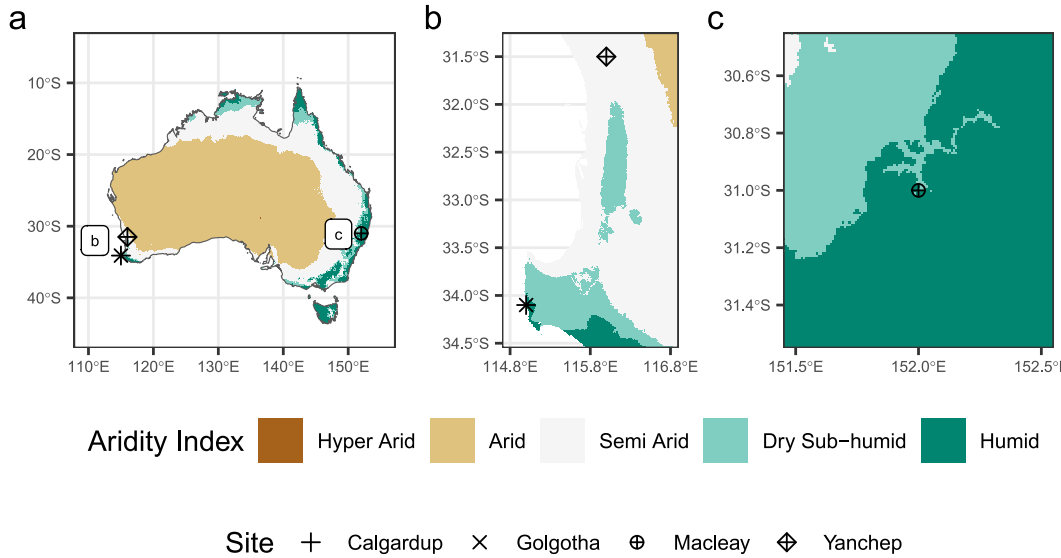

Figure 1. Map of Australia showing the four ash collection locations. The aridity index is also mapped according to Zomer et al. (2022). (a) Australia, with collection sites indicated. (b) Southwest WA, with collection sites at Yanchep, Calgardup Cave, and Golgotha Cave indicated. (c) The Macleay region, with collection sites indicated. The base Australia map is the GEODATA TOPO 250K Series 3 (Geoscience Australia, 2006).

deposition, while others have suggested that the ash bed is not a source of PAHs for soils, and that PAHs are instead mobilized and transported to waterways rather than infiltrating (Kim et al., 2011; Simon et al., 2016).

Speleothems are excellent geochemical archives of past surface environmental change (e.g., Cheng et al., 2016; Domínguez-Villar et al., 2009). While speleothem proxies have recently been used to investigate past fires (see Argiriadis et al., 2023; Homann et al., 2022, 2023; McDonough et al., 2022), a process-based understanding of the formation of fire proxies (both organic and inorganic) and how they reflect fire activity is needed to (a) build confidence in speleothems as archives of past fire, and (b) determine whether and how speleothems can record past fire severity as well as frequency. Here we present analyses of inorganic proxies in the water-soluble fraction of ash and soil samples collected from southwest and southeast Australia, and organic pyrogenic biomarkers from the solvent-extracted fraction of ashes. We present a suite of elemental data, as well as electrical conductivity (EC), pH, and alkalinity for ash and soil leachates, and a limited number of pyrogenic biomarkers for a subset of ash samples. The results presented here will aid the interpretation of both organic and inorganic palaeofire proxy data in natural archives such as speleothems and sediment cores. Understanding wildfire ash chemistry in the karst environment also has implications for water resource planning and contamination risk management.

2. Site Description and Methods

2.1. Site Descriptions

2.1.1. Southwest Australia

We collected ash and soil samples from two regions in southwest Australia: Yanchep National Park in the Perth region and Leeuwin-Naturaliste National Park in the Capes region (Figure 1). Yanchep National Park (hereafter, "Yanchep" or "the National Park") is located ~47 km north of Perth, Western Australia. The underlying geology is the Tamala Limestone, a Pleistocene aeolianite (Playford et al., 1976). The climate is characteristically Mediterranean, with cool, wet winters and hot, dry summers, with most rainfall occurring during the winter (McDonough et al., 2022). Vegetation in the region generally follows a progression inland from dune vegetation dominated by sedges, rushes, and rhizomatous grasses to coastal heath, limestone heath, and then *Banksia*-dominated woodland, with some wetland present (Fontaine, 2022). Eucalypt and *Melaleuca* woodlands are also widespread. Ash samples were collected at Yanchep between 6–8 January 2020, following a severe wildfire between 11–15 December 2019 in a region of the National Park where vegetation is comprised of a tuart (*Eucalyptus gomphocephala*) overstorey with an understorey of *banksia* heath, interspersed by occasional

wetland. The 2019 fire burned ∼12,300 ha, but with some variability, such that a range of burn severity classes are represented (Fontaine, 2022). An analysis of the differenced Normalized Burn Ratio (dNBR; see Text S1 in Supporting Information S1) shows that the most common severity class was "Moderate-high severity", representing ∼5,200 ha (dNBR between 0.44 and 0.659; Key & Benson, 2006). See Text S1 in Supporting Information S1 for a dNBR map of this event. 1.6 mm of precipitation was recorded at the nearest BOM weather station (Gingin, station number 9178, >18 km from the site) in the interval between the fire and the sample collection. Soil samples were collected from two sites within Yanchep National Park in 2022, see Section 2.3 for the sampling protocol.

Both ash and soil samples were collected from above the Calgardup and Golgotha caves in the Capes region of southwestern Western Australia, between Cape Leeuwin and Cape Naturaliste (Figure 1). As for Yanchep, the underlying geology is Tamala Limestone, and the climate is also Mediterranean, although annual precipitation is higher, and temperatures are more moderate than at Yanchep. The vegetation community at Golgotha Cave is eucalypt open forest characterized by a mixed canopy of marri (*Corymbia calophylla*) and jarrah (*E. marginata*) with occasional karri (*E. diversicolor*) on the ridge above the cave, and tall open karri forest below the cave. The understorey is a mixture of *Agonis flexuosa*, *Trymalium spathulatum*, *Podocarpus drouynianus*, *Xanthorrhoea preissii*, *Bossiaea disticha*, and *Templetonia retusa* (Treble et al., 2016). The Golgotha Cave ash samples were collected from above the cave on 14 January 2022, following a wildfire that ignited on 8 December 2021 and which burned nearly 8,000 ha in the Leeuwin-Naturaliste National Park (DBCA-060 Fire History database; https://catalogue.data.wa.gov.au/dataset/dbca-fire-history). Of those ∼8,000 ha, ∼5,400 ha are classified by dNBR as being of "High Severity" (dNBR >0.66; Key & Benson, 2006), and ∼1,400 ha classified as "Moderate-high severity." See Text S1 in Supporting Information S1 for a dNBR map of this event. The nearest BOM weather station (Forest Grove, station number 9547, ∼3.8 km from the site) recorded 5.4 mm of precipitation in the interval between the fire and ash sampling.

Dominant vegetation at Calgardup Cave is a low open forest of jarrah and marri with a dense and diverse understorey comprised mainly of *Banksia*, *Xanthorrhoea*, *Hakea*, and *Melaleuca* species close to the cave entrance, but which grades into a mix of marri-jarrah and karri to the southwest. The Calgardup Cave ash samples were collected from above the cave in August 2018, one day after a low-intensity prescribed burn. The fire was small, highly localized, and cloud cover was too heavy for dNBR analysis of this event. However, the post fire condition showed that no canopy was burnt, indicating that severity was overall low. 0.7 mm of precipitation was measured at Calgardup after the prescribed burn but prior to ash sample collection. Soil samples were collected opportunistically from above both the Calgardup and Golgotha caves, and from six other sites in the Leeuwin-Naturaliste National Park between 2006 and 2022.

2.1.2. Southeast Australia

Ashes were collected from the Macleay Karst Arc located in the Mid North Coast of New South Wales (NSW), southeast Australia (Figure 1). The underlying geology is a Permian limestone comprising a basal calcareous mudstone, a central unit of crinoidal limestone, and discontinuous reef limestones (NSW Department of Environment, Climate Change and Water, 2011). The climate is temperate humid sub-tropical, with strong temperature seasonality, and a seasonal bias in precipitation with most precipitation occurring in summer (Baker et al., 2020). Vegetation is varied, with some subtropical rainforest interspersed with cleared areas. Ash samples were collected on 1 February 2020 following the Carrai East fire, which burned from October 2019 to January 2020 during the Australian "Black Summer" fire season. The fire burned ∼150,278 ha (NSW Rural Fire Service, 2020). dNBR analyses suggest that this includes ∼42,000 ha burned at high severity, and ∼75,000 ha burned at moderate-high severity, noting that the unusual length of the event (2 months) may have skewed the dNBR results (see Text S1 in Supporting Information S1). The closest BOM weather station (Toorooka (Moparrabah), station number 59055, ∼5 km from the site) recorded 47 mm of precipitation between 8 November 2019 and sample collection, noting that after the 31 December 2019 the station was not functional. The second closest BOM weather station (Bellbrook, station number 59122, ∼15 km from the site) recorded 122 mm of precipitation between fire ignition and sample collection, noting that reported data for the entire period is not quality assured. No soil samples were collected from southeast Australia, as the site was not accessible due to extensive flood damage in 2022 following the fires in 2019/2020.

2.2. Fire Histories

Fire histories for each site were extracted from databases. The Western Australian Department of Biodiversity, Conservation, and Attractions maintains a spatial data set of known fires in Western Australia (DBCA-060 Fire History), with fire event polygons, fire type, fire size, and approximate dates, among other fields (https://catalogue.data.wa.gov.au/dataset/dbca-fire-history, accessed November 2022). The earliest fires recorded in the database are from 1937, and known issues include missing events and inaccurate dating (Dixon et al., 2022). The NSW National Parks and Wildlife Service (NPWS) maintains a data set of wildfire and prescribed burn events which occurred within the NPWS estate as well as some fire events which occurred or extended beyond the estate (NPWS Fire History—Wildfires and Prescribed Burns; https://datasets.seed.nsw.gov.au/dataset/fire-history-wildfires-and-prescribed-burns-1e8b6, accessed in November 2022). The database includes fields which describe the fire extent and type of fires which have occurred since 1920, and was last revised in October 2022.

The two fire history databases were interrogated using *QGIS (3.28.0)* and *R (version 4.3.1),* with the *dplyr (1.1.2)*, *sf (1.0.14)*, and *rgdal (1.6.7)* packages (Bivand et al., 2021; Pebesma, 2018; QGIS Development Team, 2022; R Core Team, 2023; Wickham et al., 2020), and fire histories for each ash and soil sampling location were extracted. Scripts detailing this process are available in the supplementary data set (M. Campbell et al., 2024). These fire histories are represented in the data set as two variables—the number of years since the last fire prior to collection (i.e., the penultimate fire for ash samples), and the total number of fires experienced for each sample location prior to collection. Some manual corrections were made to the fire histories where the spatial resolution of the database was insufficient to accurately delineate between burned and unburned sites at the fire edge. Where the location had not experienced a fire during the observational period (i.e., 8 of the 9 Macleay samples), the years since the last fire was given as 100 years, the length of the NPWS database.

For the length of the fire history databases, most sample sites had experienced at least one fire during the observational period, with a median number of fires of four and a maximum of nine. Of the sampling sites, Macleay sites had had the fewest total fires, Yanchep sites had experienced between three and nine fires, Golgotha Cave experienced between four and five fires, and Calgardup Cave had five recorded fires.

The median period since the last fire for all sample locations was 14 years, and 88% of sample locations had burned in the 50 years prior to collection. For the ash samples, sample sites above Calgardup Cave and at Yanchep had burned most recently (years since previous fire were 10 and 14 years, respectively). Sample locations above Golgotha Cave were last burned 16 years before sample collection. Most Macleay sample locations had no recorded fires, but one sample site had burned 18 years prior to sample collection.

2.3. Sampling Protocols

Forty-three ash samples were opportunistically collected from the ground surface following fire events at the sites described above. Ash samples were collected one day after the fire at Calgardup Cave, ∼1 month post-fire at Golgotha Cave and Yanchep National Park, and within 3 months of the fire at Macleay. Ashes were classified according to a simple color classification: black, gray, red, and white (Figure 2). Ash sampling was targeted for inorganic analyses in the first instance. Plastic equipment was used to collect and store the samples to avoid contamination with metals. At Golgotha Cave (the most recent site sampled), a duplicate data set was collected specifically for organic geochemistry analyses. These samples were collected using metal implements and stored in aluminum foil to minimize plastic contamination. A limited number of samples from Yanchep, Calgardup Cave, and Macleay, which were collected with the inorganic sampling protocol, were subsequently also analyzed for lipid biomarkers. Samples collected for inorganic analyses were stored in plastic zip loc bags in a cool storage room. Samples collected for organic analyses were stored in aluminum foil in a cool storage room.

Ash samples are not evenly distributed by either site or ash color. A greater number of samples were collected at Yanchep, with the fewest samples collected at Calgardup Cave (Figure 2). More gray and black samples ($n = 17$ and $n = 16$, respectively) were collected than red and white samples ($n = 1$ and $n = 9$; Figure 2). This is due to the opportunistic nature of sampling, which largely relied on volunteer efforts.

A total of 44 soil samples were collected from 10 sites in southwest Australia in 2006, 2015, and 2022. The 2006 and 2015 sampling targeted the Capes region sites, while 2022 sampling targeted both the Capes region and Yanchep National Park (see Table S1 in Supporting Information S1 for a list of soil sampling locations). The 2006 samples collected from above Golgotha Cave were collected as part of sample collection for Treble et al. (2016),

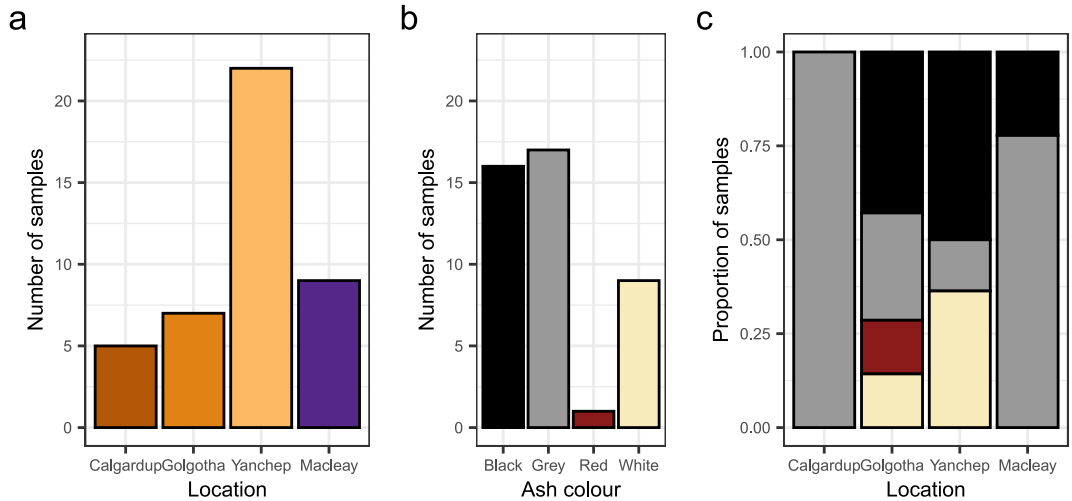

Figure 2. Distribution of ash samples by location (a), ash color (b), and both location and ash color (c).

while 2015 Capes region samples were targeted at sites that had experienced recent fires (e.g., Moondyne in 2003) and sites which had not burned in decades (e.g., above Jewel Cave which last burned in 1961). 2022 sampling was undertaken on sites which had burned in recent years at both Yanchep and in the Capes region, some of which had previously been sampled in 2006 and/or 2015. Sampling protocol was to collect soil at depths of 0–10 and 10–20 cm (for one sample only the top 5 cm of soil was collected). Samples collected in 2006 were collected from the vertical face of a large pit. While metal implements were used in the pit excavation and bulk sample collection, the large samples (1–2 kg) minimize any potential contamination. Samples collected in 2015 and 2022 were taken with a plastic trowel from small pits to minimize metal contamination. In all instances, care was taken to minimize the mixing of surface and subsurface soils, and all samples were stored in plastic sample bags. For statistical analyses, all samples were categorized as sampled from 0–10 or 10–20 cm. Samples were not evenly selected by site or location, with a larger number of samples collected from the Capes region than from Yanchep. More than 20% of the samples were collected at Golgotha Cave.

2.4. Inorganic Analyses

Inorganic geochemistry was undertaken on all ash and soil samples at the Isotope Tracing in Natural Systems laboratory at ANSTO, Lucas Heights, Australia. Ash leachates were extracted from unhomogenized samples using the USGS field leach test (Hageman, 2007). The sample was mixed with deionized water at a ratio of 1:20 by weight, agitated for 15 min, and then rested for 10 min. The supernatant was filtered using 0.45 µm pore-size nitrocellulose filters and alkalinity and pH measurements were performed using a Metrohm 862 Compact Titrosampler following Standard Methods for the Examination of Water and Wastewater, Method 4500-CO_2 D. Carbon Dioxide and Forms of Alkalinity by Calculation (American Public Health Association, American Water Works Association, Water Environment Federation et al., 2017). EC for a subset of samples was measured by a Radiometer CDM92 conductivity meter. A sub-sample was acidified with Merck Suprapur HNO_3 to 1% (vol/vol) for cation analysis by inductively coupled plasma atomic emission spectroscopy and inductively coupled plasma mass spectrometry, and an unacidified portion was retained for anion measurement by ion chromatography (IC). For the elemental analyses, procedural blanks were analyzed and are presented in Tables S2 and S3 in Supporting Information S1. No blank corrections were performed, as most blank concentrations were less than the limit of detection (LOD).

Samples were stored in laboratory refrigeration at 4°C prior to analysis. To analyze a majority of (including volatile) elements, soil leachates were prepared as received to maintain their integrity. One batch of samples (2022/0199) was subsequently corrected for moisture content for report consistency with the other samples, as they were moist when collected—see Text S2 in Supporting Information S1 for correction equations.

The charge balance error (%) was calculated for ash and soil leachates in PHREEQC. For ash leachates, total alkalinity, pH, Ca, K, Mg, Na, Si, P, Sr, Ba, Br, F, Cl, SO_4, and NO_3 were used as the input variables, with a

temperature of 25°C. Forty-three of the 58 samples (including replicates) returned charge balance errors within ±10%, while 23 samples returned charge balance errors within ±5% (noting that the charge balance was calculated on replicates separately; see Table S4 and Figure S1 in Supporting Information S1 for charge balance errors). The largest proportion of leachates with a positive charge imbalance were from black ashes (~47% of black ash samples had a >+10% error), while only one gray ash leachate sample, and no white or red samples had a charge balance error >+10%. The positive charge imbalance for the black ash samples may be attributed to the higher proportion of organic matter typically found in black ashes (Bodí et al., 2014), which may have resulted in higher dissolved organic carbon concentrations in the leachates. This can result in organic anions contributing significantly to the charge balance. This is not accounted for in the PHREEQC charge balance calculation, which includes only inorganic ions (Dasgupta et al., 2015). Three ash leachates returned charge balance errors <−10%, two of which were <−40%. All three negatively charged leachates were samples from the Macleay region. Most Macleay samples had charge balance errors <−5% (see Table S2 in Supporting Information S1).

Charge balance error was calculated for only 27 of 63 soil leachates (including replicates) due to missing pH data. For soil leachates, the input variables were total alkalinity, pH, Ca, Fe, K, Mg, Na, P, Br, Ba, Sr, Cl, SO_4, and NO_3, with a temperature of 25°C. Twenty-two of the 27 samples returned a charge balance error within ±10%, and 11/27 returned a charge balance error within ±5% (see Table S5 in Supporting Information S1). One sample, collected at Yonderup, within Yanchep National park, returned a charge balance error of ~+39%. Due to the small sample size, and uncertainty around the charge balance of the samples which could not be calculated using PHREEQC, no data were excluded from the subsequent statistical analyses.

Preliminary analysis of a subset of the ash data (nine variables measured in 16 samples from Yanchep National Park) was previously presented as a case study in M. Campbell et al. (2023). Results presented there showed that the ash leachate chemistry differed between black and white ashes ($n = 16$). This supported the hypothesis of McDonough et al. (2022) that speleothem palaeofire trace element proxies are sourced from ash.

2.5. Biomarker Analyses

Biomass burning biomarkers (levoglucosan and PAHs) were analyzed in the GNS/VUW Organic Geochemistry Laboratory at GNS Science, New Zealand. Freeze-dried, homogenized ash (0.33–0.95 g) samples were extracted three times with dichloromethane/methanol (3:1, v:v) by ultrasonication for 20 min each time, followed by centrifugation at 2,000 rpm for 5 min. The resulting extracts were filtered on cotton wool-plugged Pasteur pipettes and evaporated under N_2 at 35°C to obtain dried total lipid extracts (TLEs). Half of each TLE was derivatized with 50 µL *N*, *O*-bis(trimethylsilyl)trifluoroacetamide (BSTFA) with 1% trimethylchlorosilane (TMCS) at 70°C for 1 hr. After cooling, the solutions were evaporated under N_2 at 35°C until dryness and redissolved in *n*-hexane for analysis.

The derivatized TLEs were analyzed by gas chromatography mass spectrometry on an Agilent 7890A GC System, equipped with an Agilent J&W DB-5ms capillary column [60 m × 0.25 mm inner diameter (i.d.) × 0.25 µm film thickness (f.t.)], and coupled through a split to an Agilent 5975C inert MSD mass spectrometer and a flame ionization detector. The temperature program of the oven was 70–130°C at 20°C min^{-1}, then at 4°C min^{-1} to 320°C and held isothermal for 15 min, which results in a total run time of 65.5 min. Helium was used as carrier gas with a constant flow of 1.0 mL min^{-1}. Samples (3 µL) were injected splitless at an inlet temperature of 300°C. The MS was operated in the electron impact ionization mode at 70 eV using a source temperature of 230°C. After a solvent delay of 10 min, the samples were analyzed in full scan mode with *m/z* 50–700.

Internal standards (5α-cholestane, *n*-nonadecanol, and *n*-nonadecanoic acid) for quantification were added to the samples prior to the first extraction. Procedural blanks and laboratory reference standards were also analyzed to ensure data quality and absence of laboratory contaminants.

Analyses of Golgotha Cave ash samples were repeated in November 2023 to test for alteration of the biomarker signal ex situ. The same sample protocol above was followed except larger sample sizes (up to 2.81 g) were used.

2.6. Software and Statistical Methods

Data were analyzed and visualized using the statistical software *R* (version 4.3.1), and the packages *readr (2.1.4)*, *dplyr (1.1.2)*, *ggplot*2 (3.4.2), *boot (1.3–28.1)*, *ShapleyValue (0.2.0)*, *stringr (1.5.0)*, *tidyr (1.3.0)*, *ggbiplot (0.55)*, *EnvStats (2.8.0)*, *purr (1.0.1)*, and *stats (4.3.1)* (Canty & Ripley, 2022; Davison & Hinkley, 1997; Liang, 2021;

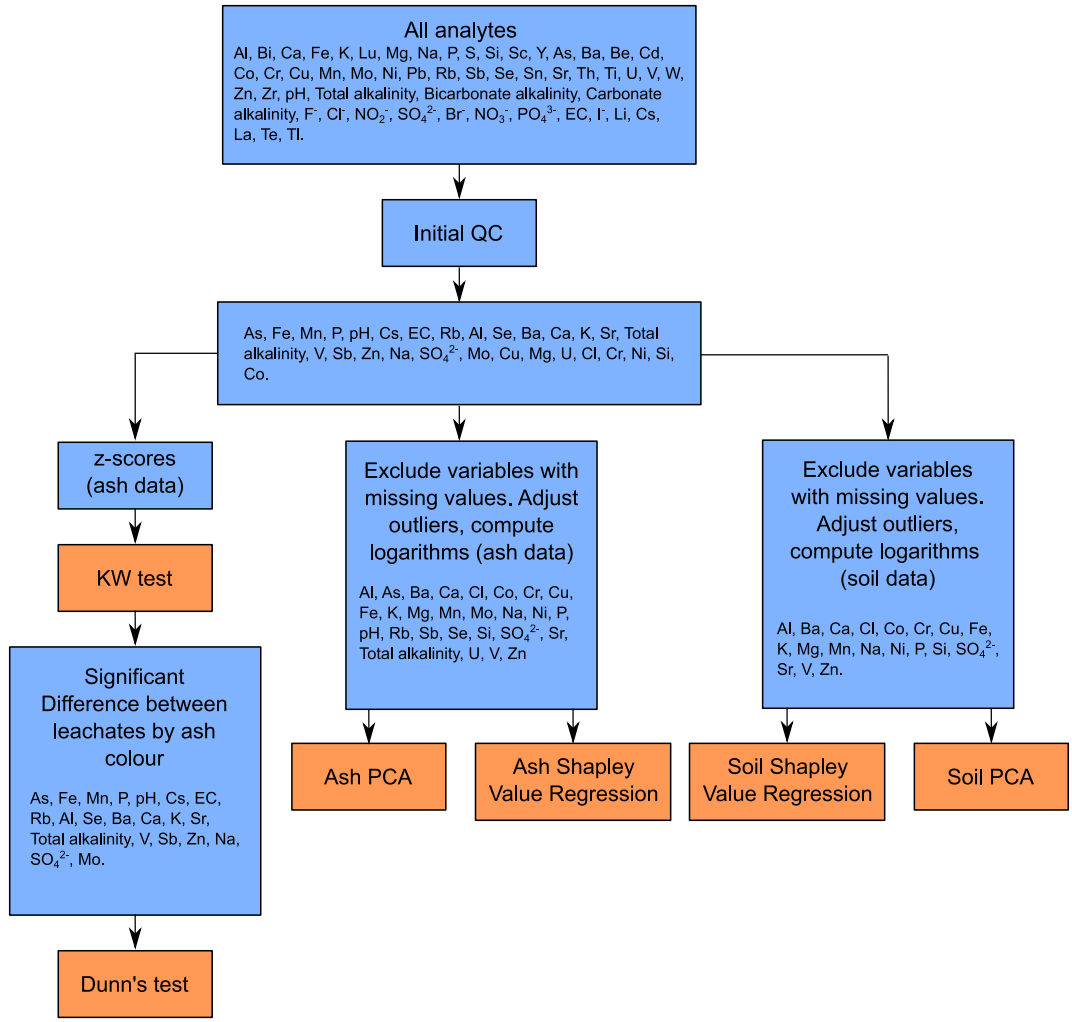

Figure 3. The workflow for the data processing and statistical analyses of inorganic leachate data. Orange boxes indicate a statistical test, and blue boxes indicate a data processing step.

Millard, 2013; R Core Team, 2023; Vu, 2011; Wickham, 2016, 2022; Wickham and Henry, 2023; Wickham et al., 2020, 2023). Fire history databases were clipped to the study sites in QGIS (*3.28.0*) before interrogation in *R* (QGIS Development Team, 2022). Figure 3 shows the data processing workflow and the analytes used for each statistical test.

Where replicate leachates were analyzed, the results were combined and the means used in the statistical analyses. Outliers in the soil and ash leachate chemistry were identified using Rosner's Test in the R package "EnvStats," which allows for multiple outliers to be identified (Millard, 2013; Rosner, 1983). Outlier identification was adapted from a script presented by Croke et al. (2021). As the sample sizes for soil ($n = 43$) and ash ($n = 44$) leachates were small, outliers were replaced with the median value rather than removed. Histograms of the data distributions for both soil and ash leachates with outliers indicated are found in Figures S2 and S3 in Supporting Information S1. Histograms show that geochemistry data are all skewed, necessitating either transformation or non-parametric statistical tests. Initial quality control was conducted to limit the number of analytes included in the statistical analyses (see Text S3 in Supporting Information S1 for details).

To test how ash chemistry changes with ash color, we applied the non-parametric Kruskal-Wallis rank sum test to determine if there was a significant difference in ash chemistry between ash colors (Hollander & Wolfe, 1973). To minimize the impact of location on the ash chemistry, data were first grouped by location and then transformed into *z*-scores. The null hypothesis of the Kruskal-Wallis test is that samples originate from the same distribution,

with the alternative hypothesis that the samples originate from different distributions. A significant Kruskal-Wallis result indicates that there is some difference in the distributions, but it cannot tell where that difference occurs. Dunn's Test is the nonparametric post hoc test for multiple comparisons (Dunn, 1964), and shows which variables are significantly different from one another. The null hypothesis is that there is no difference between groups, while the alternative hypothesis is that there is a difference between groups. Importantly, Dunn's test allows for groups to be of equal or unequal size.

Shapley Value regression allows the relative importance of predictor variables in linear regression to be calculated. It achieves this by computing the R-squared for each possible combination of predictor variables and calculating the average improvement when adding a variable to a model (Budescu, 1993; Lipovetsky & Conklin, 2001). Shapley value regression was undertaken on the ash and soil leachate data using the *ShapleyValue* package in *R* (Liang, 2021; R Core Team, 2023). For the ash samples, the predictors were ash color, location, years since the last fire, and the total number of fires. For the soil sample analyses, the predictors were sample depth, location, years since the last fire, and the total number of fires. For both ash and soil data, values were log-transformed (base 10) prior to analyses. Confidence Intervals (CIs) were calculated at $\alpha = 0.95$ using the bias corrected and accelerated intervals (BCa) on bootstrap replicates of the standardized Shapley values ($R = 5{,}000$). Bootstrap resampling and calculation of CIs were done using the *boot* package in *R* (Canty & Ripley, 2022; R Core Team, 2023). BCa intervals were used to calculate CIs as it is the only method which is guaranteed to return intervals within the statistics sampling space (0–1), and is in general recommended, given sufficient sample *n* and bootstrap replicates (Carpenter & Bithell, 2000; Puth et al., 2015)

Principal component analyses (PCA) were performed using the "*prcomp*" function in R on the logarithm (base 10) of the inorganic leachate data (R Core Team, 2023). The PCAs were performed on the correlation matrix, and data were mean subtracted. Where zeroes were introduced due to how values <LOD were handled (by replacing those values with a random number between zero and the LOD), these zeroes were replaced with the minimum measured value for that variable. Figures S2 and S3 in Supporting Information S1 show the distributions of the input data.

3. Results

3.1. Ash

3.1.1. Relationships Between Ash Color, Chemistry, and Burn Severity

We calculated the Ca/Mg ratio for each ash sample (Figure 4) and found that black ash leachates consistently have a Ca/Mg ratio greater than one (>80% of black ash samples), gray samples have a median Ca/Mg value of less than one, but 35% of samples had a ratio greater than one. While the median Ca/Mg value for white ash is slightly higher than that of gray ash (0.57 as opposed to 0.55—with an outlier of >30,000 removed from the white samples), but less variable ($\sigma = 0.266$ as opposed to $\sigma = 2.38$) and only two of nine white ash samples have a Ca/Mg value greater than one. The red ash leachate sample had a ratio comparable to that of black ash.

Ash leachate chemistry has been shown to vary with ash color, which is itself a product of combustion completeness. Here, we tested for significant differences in ash leachate chemistry between ash colors using both the Kruskal-Wallis ranked sum test and Dunn's test, which makes multiple pairwise comparisons. The results of the Kruskal-Wallis test showed that there is a significant difference in the pH, total alkalinity, EC, Na, K, Rb, Cs, Al, Mn, Fe, P, As, Se, and SO_4 (see Table S6 in Supporting Information S1 for Kruskal-Wallis *p*-values). Dunn's test for multiple comparisons shows which ash color groups are statistically different from one another. Figure 5 shows boxplots of the *z*-scores of each variable by ash color. The results of Dunn's test are labeled, showing that in general it is only the severity end members (black and white ashes) which report significantly different concentrations. Boxplots of all variables by ash color are found in Figure S4 in Supporting Information S1, and a table of mean non-normalized values for each variable is presented in Table S7 in Supporting Information S1.

Where black and white ash leachate analytes were significantly different (pH, total alkalinity, EC, Na, K, Rb, Cs, Al, Mn, Fe, P, As, and SO_4), values were higher in black than white ash leachates for Al, Mn, Fe, P, and As, while values were higher in white than black ash leachates for total alkalinity, pH, EC, Na, K, Rb, Cs, and SO_4. Despite the Kruskal-Wallis test indicating that concentrations of Se were significantly different between different colored ashes (Table S6 in Supporting Information S1), Dunn's Test found that the chemistry of the black, gray, and white ash leachates were statistically similar for these analytes. While in general the differences between the end

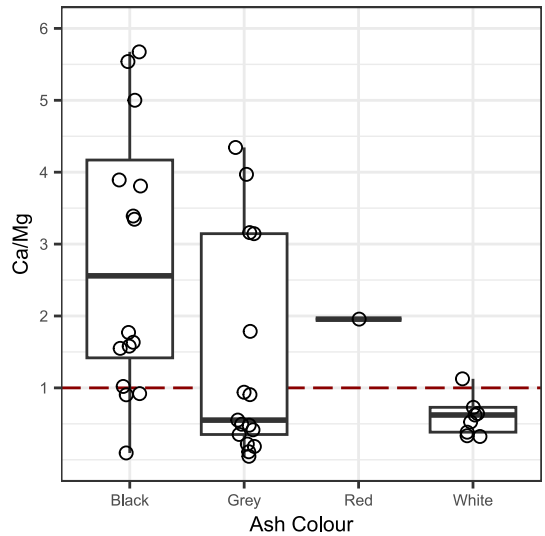

Figure 4. Boxplots of Ca/Mg ratios of ash leachates for all sites by ash color. The dashed red line indicates a Ca/Mg ratio of 1. Note that three outliers are omitted from this plot by the *y*-axis scaling—one black ash sample with a Ca/Mg value of 11.8, one gray ash sample with a Ca/Mg of ∼9.2, and one white ash sample with a value of 34,067.8 due to very low Mg concentration in that sample.

members (black and white ash) were the most significant, gray and black ashes were significantly different for pH, K, Cs, Al, Mn, Fe, P, and As. There is no evidence of statistical differences between gray and white ashes (Figure 5).

3.1.2. Predictors of Ash Leachate Chemistry

Shapley value regression is used to quantify the influence of predictor variables (see Section 2.6). Standardized Shapley regression values were calculated for each of the 27 ash leachate variables and four predictors (ash color, location, years since the last fire, and the total number of fires), with 95% CIs. Results show that ash color was the most important predictor for 11 variables (Al, As, Fe, K, Mn, Mo, Ni, P, pH, Rb, and Zn), location was the most influential predictor for 16 variables (Ba, Ca, Cl, Co, Cr, Cu, Mg, Na, Sb, Se, Si, SO_4, Sr, total alkalinity, U, and V), although there is high overlap in the 95% CIs for many analytes, particularly between ash color and location. Ash color was the dominant predictor (standardized Shapley value >0.5) of Al, As, Mn, Mo, P, and pH. Location was the dominant predictor of Ba, Ca, Cu, Sb, Se, Si, Sr, U, and V. Neither years since the last fire nor the total number of fires were the dominant predictors of any variables. The highest standardized Shapley values for years since the last fire and the total number of fires were 0.288 (Cr) and 0.319 (Mg), although these values were associated with wide CIs (see Table S8 and Figure S5 in Supporting Information S1). Noting that the Macleay ash samples were exposed to up to 122 mm of precipitation prior to sample collection and thus had a greater chance of leaching in situ, we repeated the Shapley value regression with those samples excluded (see Table S9 in Supporting Information S1). Results show reduced influence of location for the remaining sites for many analytes, and particularly for Cl, Co, Cr, Cu, Na, Se, SO_4, total alkalinity, and V, where ash color rather than location became the most important predictor. We note that for Co, Cu, Si, alkalinity, and V, there is a high overlap in the 95% CIs between ash color and location. Conversely, there is no overlap in the 95% CIs for Cl, Cr, Na, or SO_4, indicating that the change in the most important predictor is robust. Figure S6 in Supporting Information S1 shows the concentrations of analytes by sampling location, showing that concentrations of Cl, Cr, Na, and SO_4 were all lower at Macleay than at other locations.

PCA was applied to the full ash leachate data set (Al, As, Ba, Ca, Cl, Co, Cr, Cu, Fe, K, Mg, Mn, Mo, Na, Ni, P, pH, Rb, Sb, Se, Si, SO_4, Sr, total alkalinity, U, V, and Zn (Table 1)). A scree plot (see Figure S7 in Supporting Information S1) suggests that while the first three principal components (PCs) contain the most information, the first seven PCs each contain more information than if all PCs explained an equal amount of variance, and so should also be presented. Together the first two PCs account for ∼45% of the variance, and >95% of the variance is described by the first 15 PCs. Loadings can be considered to be important if they contribute more than the average amount of information to the PC. Here, that threshold is ±0.19.

Table 1 presents the loadings for the first seven PCs. Loadings and a biplot of PC1 and PC2 (Figure 6a) shows that black ash samples cluster differently to white and gray ash samples. Variables which load strongly positively on PC1 (Al, Mn) all have higher concentrations in black ash than white ash, while variables which load strongly negatively on PC1 (Cl, Cr, K, Na, pH, SO_4, Rb, and total alkalinity) are all higher in white ash than black ash, noting that the difference between white and black leachates is not statistically significant for Cl and Cr (Figure 5, Figure S4 in Supporting Information S1). The clustering of gray/white versus black ash leachates suggests that burn severity impacts ash leachate geochemistry.

Similarly, there is clear clustering of points by location, with samples from southwest western Australia and samples from southeastern Australia having little overlap in a biplot of PC1 and PC2 scores (Figure 6b), although it should be noted that the majority of Macleay samples were gray ashes. When samples are grouped by the number of years since the last fire (two groupings applied: samples below the median (14 years) or equal to and above the median), the samples clearly cluster, with sites burned less recently having more negative PC2 scores, while sites which burned more recently having more positive PC2 scores (see Figure S8 in Supporting

10.1029/2024GC011470

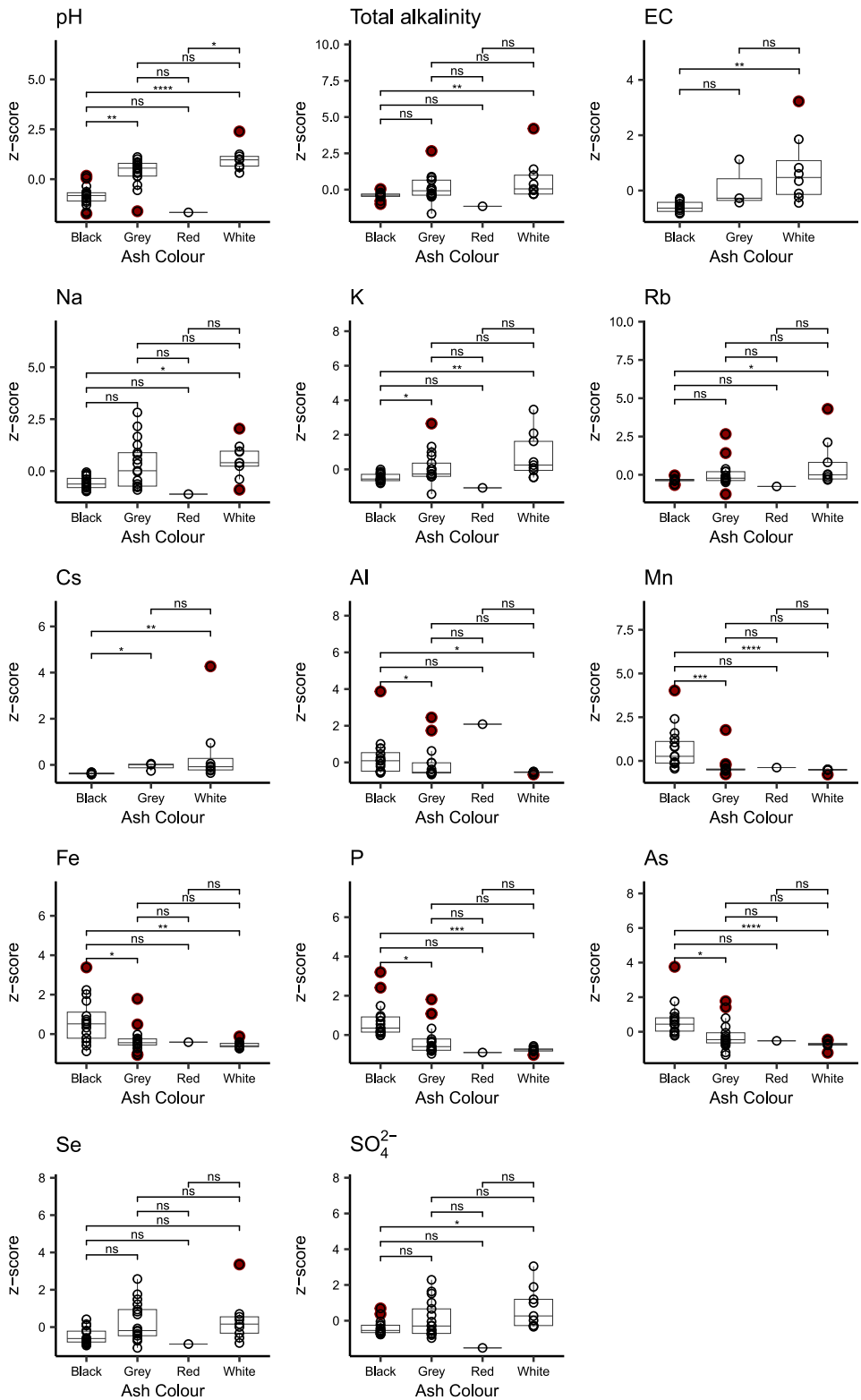

Figure 5. Boxplots showing z-scores of ash leachate elemental concentrations, electrical conductivity, pH, and alkalinity. The results of Dunn's test are also indicated. ns indicates the results are not significant, * indicates significance at $\alpha = 0.05$, ** significant at $\alpha = 0.01$, *** significant at $\alpha = 0.001$, **** significant at $\alpha = 0.0001$. Red points indicate outliers.

Table 1
Loadings for the First Seven Principal Components (PCs) From the Principal Component Analyses of Ash Leachate Data

	PC1	PC2	PC3	PC4	PC5	PC6	PC7
Al	**0.22**	−0.15	0.16	−0.12	0.09	**−0.29**	0.19
As	0.19	**−0.23**	**0.27**	−0.03	0.09	−0.19	−0.14
Ba	−0.05	**−0.39**	**−0.21**	0.09	−0.03	0.12	−0.01
Ca	0.05	**−0.32**	−0.17	0.09	−0.13	**0.43**	−0.16
Cl	**−0.29**	−0.13	0.06	−0.11	0.19	−0.02	0.05
Co	0.08	−0.10	**0.26**	0.15	**−0.42**	0.15	−0.02
Cr	**−0.24**	−0.02	0.03	**−0.28**	−0.17	**−0.24**	0.01
Cu	0.06	0.11	**0.21**	−0.04	**−0.36**	**0.30**	**0.46**
Fe	0.15	−0.12	**−0.21**	**−0.23**	0.11	**0.23**	**0.48**
K	**−0.31**	−0.06	0.08	−0.11	0.05	0.04	−0.04
Mg	−0.16	−0.18	0.19	0.05	**0.34**	**0.24**	**0.26**
Mn	**0.25**	−0.15	0.14	**−0.25**	−0.07	−0.17	0.01
Mo	−0.17	0.11	**0.21**	−0.03	**−0.37**	−0.06	−0.17
Na	**−0.30**	−0.11	0.02	−0.11	0.11	−0.06	0.09
Ni	0.05	−0.05	**0.41**	−0.19	−0.05	**0.30**	−0.07
P	0.18	**−0.23**	**0.30**	**−0.20**	0.06	−0.15	0.13
pH	**−0.23**	**0.27**	−0.08	0.07	−0.18	−0.14	0.15
Rb	**−0.32**	−0.06	0.02	−0.11	−0.03	−0.04	0.07
Sb	−0.10	0.05	**0.37**	**0.26**	0.14	**0.25**	−0.09
Se	−0.10	**0.30**	**0.20**	−0.01	**0.23**	0.17	−0.14
Si	−0.05	**−0.20**	0.13	**0.43**	−0.08	−0.11	−0.04
SO_4	**−0.30**	−0.11	0.02	−0.18	−0.04	0.09	0.01
Sr	−0.10	**−0.39**	**−0.20**	0.07	−0.03	0.05	−0.18
Total alkalinity	**−0.30**	−0.04	0.06	−0.13	−0.02	0.00	0.11
U	−0.15	**−0.27**	0.02	0.09	**−0.37**	**−0.22**	0.10
V	−0.09	−0.13	**0.23**	**0.41**	**0.23**	**−0.25**	0.15
Zn	0.02	−0.09	0.09	**−0.37**	0.05	0.08	**−0.47**
Cumulative proportion of variance	0.29	0.45	0.58	0.65	0.72	0.77	0.8

Note. Bold indicates which variables have a greater proportion of influence on the PC (threshold of ±0.19).

Information S1). Biplots of the first three PCs for the total number of fires show no distinct clustering (see Figure S9 in Supporting Information S1).

3.1.3. Ash Biomarkers

Thirteen samples from four locations (Golgotha Cave, Calgardup Cave, Macleay, and Yanchep) were analyzed, with six PAHs (Phenanthrene, Anthracene, Pyrene, Chrysene, Benzanthracene, and Benzopyrene) and levoglucosan detected. Samples from Calgardup Cave and Macleay had no measurable PAHs or levoglucosan, and samples from Yanchep had no measurable PAHs, and concentrations of levoglucosan were low (see Table S10 in Supporting Information S1). As such, only ash samples from Golgotha Cave are presented here. Concentrations are normalized to the dry weight of ash.

In general, total concentrations of the low molecular weight compounds (Anthracene, Phenanthrene, and Pyrene) were higher than for higher molecular weight PAHs (Chrysene, Bezanthracene, and Benzopyrene). PAH concentrations were generally higher in black and gray than white ash samples, particularly in the lowest molecular weight compounds, noting however that the variability for the black ash leachates is high for each PAH (Figure 7

10.1029/2024GC011470

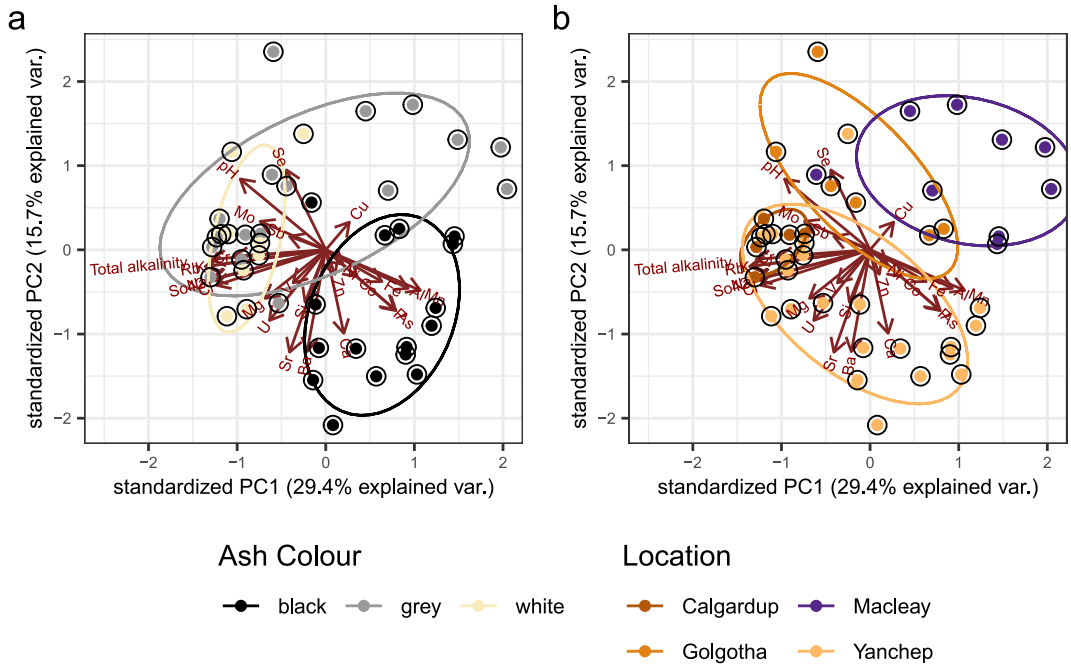

Figure 6. Biplots of standardized scores from principal component analyses of ash leachate samples. Panel (a) presents PC1 plotted against PC2, with ash color shown as both clusters and the point color. Panel (b) also shows PC1 plotted against PC2, with sample location indicated by point color and clustering.

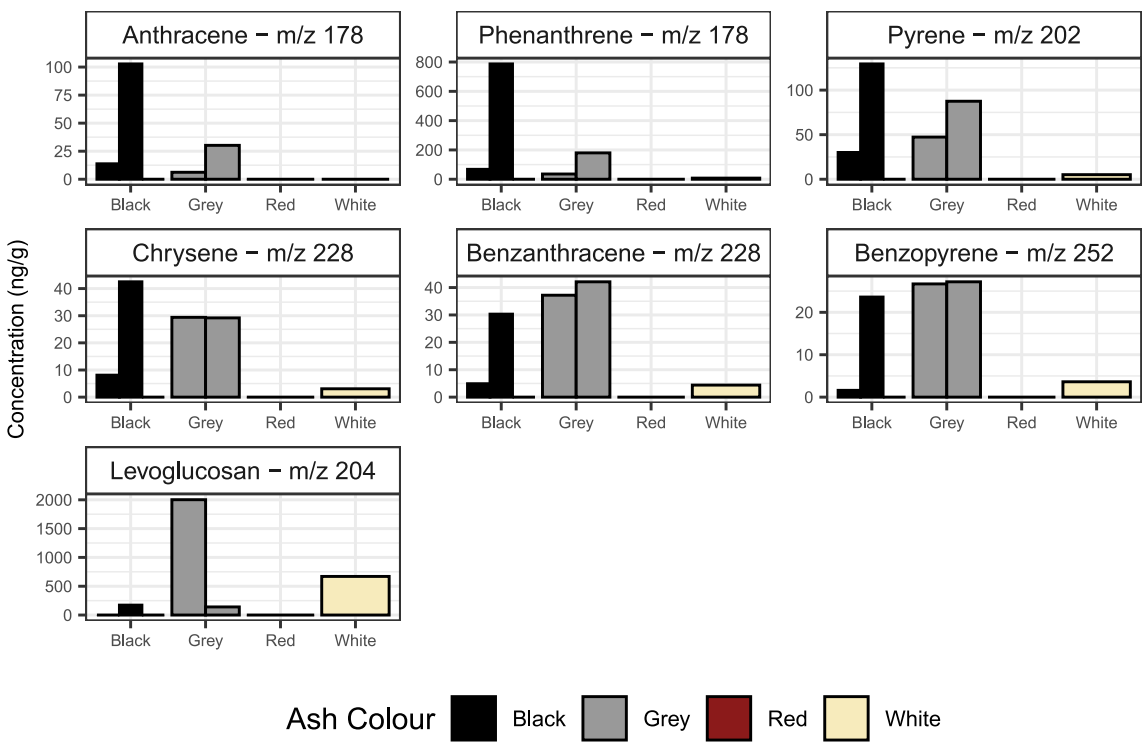

Figure 7. Concentrations of polycyclic aromatic hydrocarbons (PAHs) and levoglucosan by ash color. PAHs are arranged by molecular weight. Note that the scale of the *y*-axis is different for each plot.

Table 2
Loadings for the First Five Principal Components (PCs) of Soil Leachate Chemistry

	PC1	PC2	PC3	PC4	PC5
Al	**0.25**	−0.05	**−0.31**	−0.08	**−0.50**
Ba	**0.26**	0.10	0.14	**0.31**	−0.01
Ca	**0.34**	0.17	0.20	0.18	**−0.24**
Cl	0.00	**0.40**	−0.13	**−0.30**	0.04
Co	**−0.29**	**0.24**	−0.13	0.09	−0.08
Cr	−0.22	−0.01	**−0.40**	0.04	**−0.41**
Cu	**−0.26**	**0.28**	0.07	0.08	0.04
Fe	0.10	−0.19	**−0.51**	0.12	−0.14
K	0.06	**0.36**	**−0.35**	0.06	0.12
Mg	**0.26**	**0.27**	0.02	0.23	−0.22
Mn	**0.25**	−0.12	**−0.24**	−0.05	**0.33**
Na	0.21	**0.33**	−0.03	**−0.34**	0.11
Ni	**−0.24**	**0.24**	0.00	**0.26**	0.07
P	0.13	0.16	−0.20	**0.43**	**0.26**
Si	0.11	0.14	**−0.30**	−0.01	**0.39**
So42	0.17	0.23	0.06	**−0.50**	−0.11
Sr	**0.36**	0.15	0.20	0.12	−0.16
V	**−0.25**	0.18	−0.06	−0.13	−0.17
Zn	−0.23	**0.29**	0.15	0.17	−0.16
Cumulative proportion of variance	0.27	0.48	0.58	0.69	0.75

Note. Bold indicates which variables have a greater proportion of influence on the PC (threshold of ±0.23).

and Table S10 in Supporting Information S1), and that one black sample (Golgotha_6) had no measurable PAHs (Table S10 in Supporting Information S1). No PAHs were found in the red ash sample.

Levoglucosan had a maximum concentration of 2.0 μg/g, and a mean concentration of 0.43 μg/g (Figure 7, Table S10 in Supporting Information S1). Three (two black and one red) of the seven ash samples contained no measurable levoglucosan (see Table S10 in Supporting Information S1). Of the four Golgotha Cave samples with measurable concentrations, gray, and white samples generally had higher concentrations than black samples (Figure 7).

3.2. Soil

Standardized Shapley regression values for 17 measured variables and four predictors (location, the number of years since the last fire, the total number of fires, and the sample depth) showed that location had the most explanatory power for all variables in soil leachates (see Table S11 in Supporting Information S1). There was no overlap in the 95% CIs between location and the other predictors for any analyte except Si, where CIs for depth, years since last fire, and total number of fires slightly overlapped with those for location (see Table S11 and Figure S10 in Supporting Information S1). This suggests that for most variables sample location clearly has the greatest influence.

PCA was repeated on the soil leachates using the same variables as for the PCA of ash leachates in Section 3.1 but with the exclusion of As, Mo, pH, Rb, Sb, Se, total alkalinity, and U due to missing data (Table 2). A scree plot (see Figure S11 in Supporting Information S1) suggests that while the first two PCs explain the most variance, the first five PCs each explain an above-average proportion of the variance, and should be presented. Together, the first two PCs explain ∼48% of the variance, and >95% of the variance is explained by the first 13 PCs. Following Section 3.1, the threshold for loading "importance" is ±0.23. Table 2 presents the loadings for the first five PCs. Variables which load strongly positively on PC1 (Al, Ba, Ca, Mg, Mn, Sr) are all variables which tend to be higher in the Yanchep region than in the Capes region, and which are higher at sites which have experienced more fires. Similarly, the variables which load strongly negatively on PC1 (Co, Cu, Ni, and V) are all lower for samples from the Yanchep region, and for samples which have experienced more fires. This is illustrated in a biplot of PC1 and PC2 (Figure 8).

Cl, Co, Cu, K, Mg, Na, Ni, and Zn load strongly positively on PC2, while no variable loads strongly negatively. A biplot of PC1 and PC2 with scores colored by the distance to the coast (Figure 9) suggests that PC2 reflects proximity to the coast, with higher Cl, K, Mg, and Na in samples with higher exposure to sea spray (Davies & Crosbie, 2018).

Figure 10 compares ash and soil leachate data for sites where both ashes and soils were collected (Calgardup Cave, Golgotha Cave, and Yanchep). Ash leachates have higher pH and alkalinity than soil leachates at all sites. Elemental concentrations are generally higher in ash leachates than soil leachates at two or more sites for all elements, barring Fe, Al, and Cr. Concentrations of Fe are higher in soil leachates than in ash leachates at all sites. Concentrations of Al and Cr in soil leachates either exceed or are comparable to ash leachates (except for Calgardup Cave, where soil leachate Cr concentrations are very low). Concentrations of Na, K, Rb, Mg, Ca, Sr, Ni, Mo, P, Se, Cl, and SO_4 in ash leachates clearly exceed concentrations in soil leachates at all sites. Mn concentrations are generally higher in ash leachates at Golgotha Cave and Yanchep but are comparable to soil leachates at Calgardup Cave. Concentrations of Ba, V, Co, Cu, Zn, Si, Sb, and U are higher in ash leachates than in soil leachates for Calgardup Cave and Yanchep samples, but are comparable in Golgotha Cave samples. A table of median soil leachate concentrations is found in Table S12 in Supporting Information S1. Concentrations of Al, Cl, Cr, and Fe were higher in leachates of deeper soils than in shallower soils (see Table S13 in Supporting Information S1).

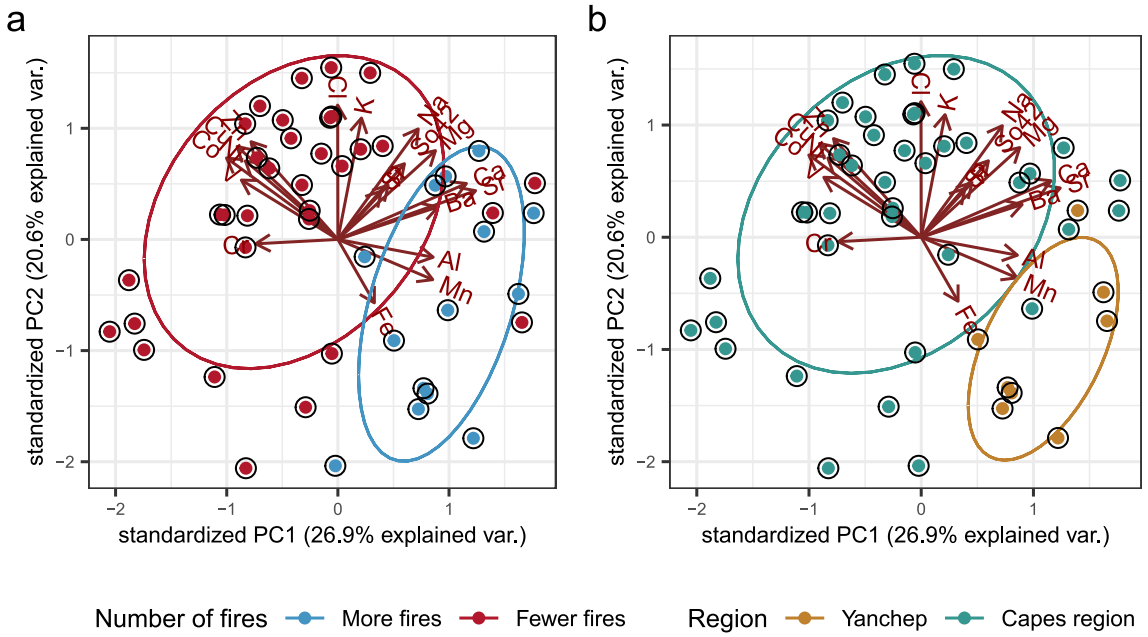

Figure 8. A biplot of soil leachate principal component analyses PC1 and PC2, with scores colored by the number of fires (a) and the region (b).

4. Discussion

Overall, our results show that inorganic ash leachate chemistry varies with burn severity (as indicated by ash color) and location, and that the past fire history (i.e., the total number of fires for each site, and the number of years since the last fire for each site) had a more limited effect on ash leachate chemistry. Ash leachate pyrogenic biomarker results were variable, and the relationship between ash color and biomarker concentrations was not clear. Soil leachate chemistry was shown to vary between sites, and as for ash leachates, the fire history had minimal impact on soil leachate chemistry. Ash leachates were generally shown to be more enriched in a range of analytes compared to soil leachates.

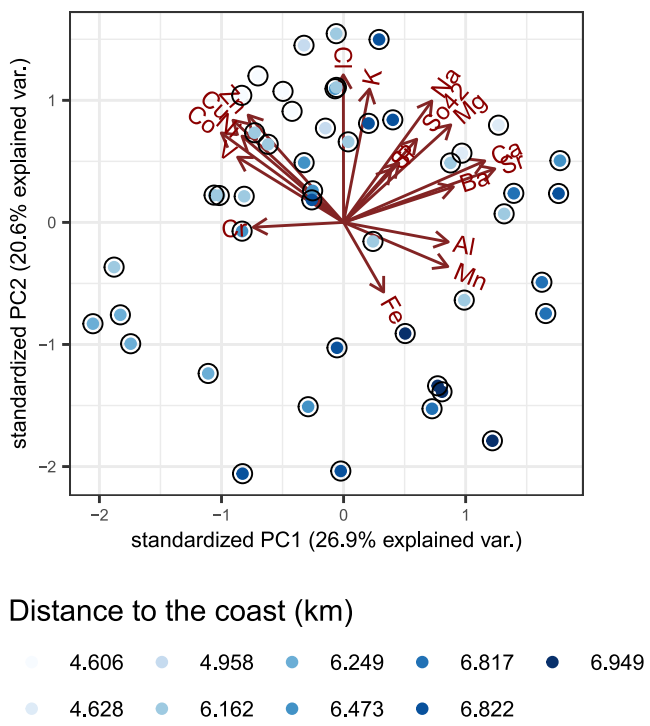

Figure 9. Biplot of soil principal component analyses PC1 and PC2, with scores colored by the distance from sample location to the coast (in km).

4.1. Ash and Soil Leachate Chemistry

4.1.1. General Ash Leachate Chemistry

Of the 29 measured variables which met the threshold for inclusion (≥25% of ash samples >LOD), SO_4, K, Cl, Na, and Ca were the most abundant elements in ash leachates, while U, Sb, Co, Cr, and Se were the least abundant elements. The elevated SO_4, K, Cl and Na values in ash leachates are likely due to higher exposure of vegetation to sea spray, with all Western Australian ash samples collected within 8 km of the coast and downstream of the dominant southwesterly winds. This is also reflected in the soil leachate data, where PC2 reflected sea spray inputs and where the most abundant elements are Na, Cl, K, Ca, and SO_4 (Figure 10).

Our analyses of ash leachates from karstified limestone environments found Na to be the most abundant element, followed by Ca and Mg. These findings are broadly consistent with a recent global analysis of wildfire ash leachate data, which showed Na, Ca, and Mg to be the most abundant (Ca > Na > Mg) (Sánchez-García et al., 2023). The predominance of Na in our samples again likely reflects the strong marine influence at our southwest Australian sites. The global analysis also showed that wildfire ash leachates were least abundant in F, Mn, and Fe, which is also in broad agreement with our results.

10.1029/2024GC011470

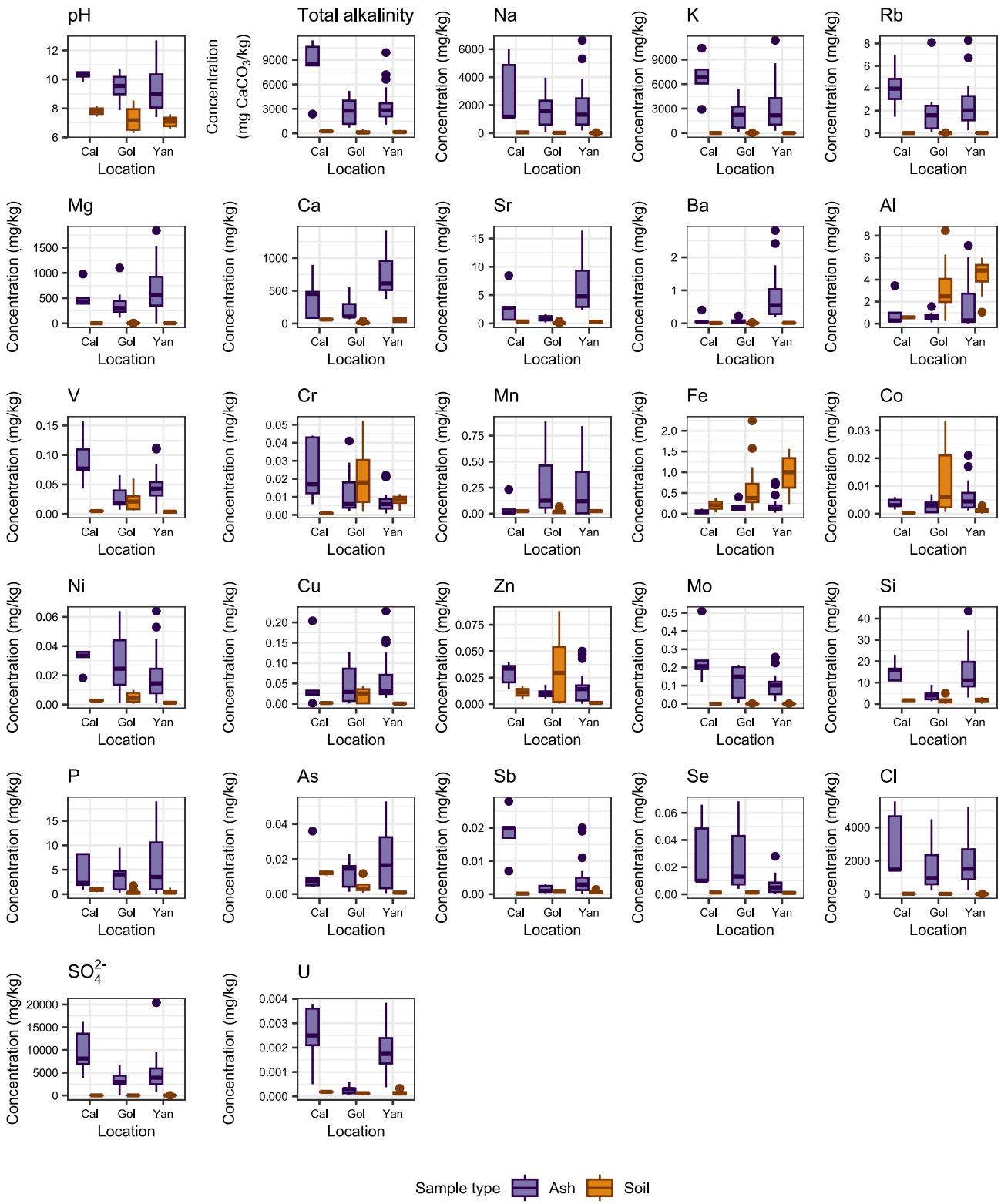

Figure 10. Boxplots of ash leachate (purple) and soil leachate (brown) chemistry for each site where both soils and ashes were collected (Calgardup Cave, Golgotha Cave, and Yanchep).

Ash leachate concentrations presented here were generally higher than the "temperate eucalypt forest" ash leachates from southeast Australian forests reported by Sánchez-García et al. (2023). However, Fe and Mn are exceptions; our results show that these elements were both lower in concentration and outside the range of data presented by Sánchez-García et al. (2023).

4.1.2. Ash Leachate Chemistry Changes With Burn Severity

Several studies have suggested that there is a relationship between combustion completeness and the Ca/Mg ratio, and a ratio <1 is thought to indicate severe burning (Marion et al., 1991; Úbeda et al., 2009). Broadly, our results support the hypothesis that a Ca/Mg ratio <1 indicates severe burning, particularly for the combustion end-members (black and white ash), but considerable spread in the data remains. This uncertainty is consistent with other studies. Úbeda et al. (2009) in a laboratory study of *Quercus suber* ash found that the relationship between the Ca/Mg ratio and combustion completeness only held for one site. While this ratio would require Ca concentrations to decrease with burn severity and Mg concentrations to increase with burn severity (or for one of these to not change with burn severity), the Kruskal-Wallis test found no statistical difference in the concentrations of these analytes between ash colors. However, a qualitative assessment of the data (see Figure S4 in Supporting Information S1) shows that in general, Ca concentrations are lower in white leachates than black ash leachates, while Mg concentrations are higher in white ash leachates. The lack of statistical difference between the concentrations of these analytes by combustion completeness is consistent with the literature, where they are generally reported to behave similarly (Balfour & Woods, 2013; Miotliński et al., 2023; Pereira et al., 2012; Úbeda et al., 2009), although Sánchez-García et al. (2023) reported that Ca concentrations were higher in ash leachates produced from severe burning, and that Mg concentrations did not vary with burn severity. The charge imbalances of the leachates also support the hypothesis that black ashes are less-combusted than white ashes. The more-positive charge balance error in black ashes was attributed to their higher levels of organic matter, which can contribute anions that are unaccounted for by our charge balance calculations.

Our hypothesis that ash leachate chemistry will change with burn severity is supported by the Kruskal-Wallis rank sum test and post hoc Dunn's test, which showed that pH, total alkalinity, EC, Cs, Rb, K, Na, and SO_4 increased with combustion completeness, while As, Fe, Mn, P, Al, and Zn decreased with combustion completeness. The Shapley value regression and PCA also indicated that ash color (representing combustion completeness) is a key control on ash leachate chemistry. Note that in both Dunn's test and the PCA, there was no statistical difference between gray and white ashes in any variable (Figure 5). This suggests that it is only the severity end-members (more completely burned vs. less completely burned) that can be distinguished in these analyses. We found no statistically significant difference in the water extractable proportion of Se, Ba, Ca, Sr, V, Sb, Mo, Cu, Mg, U, Cl, Cr, Ni, Si or Co by ash color.

A comparison of our results with the literature is presented in Text S5 in Supporting Information S1. While a review of the literature broadly indicates that ash chemistry changes with burn severity, there is considerable heterogeneity of results, suggesting that there is a spatial and perhaps methodological influence on how ash geochemistry changes with burn severity. There is better agreement between studies of the water-extractable component of ash leachates (e.g., Burton et al., 2016; Miotliński et al., 2023; Pereira et al., 2012; Quintana et al., 2007; Sánchez-García et al., 2023; Úbeda et al., 2009), with acid-digested samples tending to be less consistent. In general, our results show strong agreement with Miotliński et al. (2023) for leachate data from combustion simulation experiments conducted on soils and vegetation litter from southwestern Western Australia, see Table S5.1 in Text S5 in Supporting Information S1.

If volatilization temperature was the sole control on element concentration, we would expect to see concentrations of elements with high volatilization temperatures (e.g., Mn, Al, Zn, K, P, Cu, Mg, Ca and Na, which all volatilize at >700°C. Please see summary figures in M. Campbell et al. (2023) and Bodí et al. (2014)) in greater relative proportions in white ash than in black ash. This is true for Na and K, which are higher in white ash leachates than in black ash leachates, but Mn, Al, P, and Zn are higher in black ash leachates than in white ash leachates, and Cu, Mg, and Ca concentrations do not vary significantly with ash color. Volatilization temperatures reported in the literature are largely based on empirical combustion studies with varying experimental designs. Additional factors which may impact ash leachate chemistry beyond volatilization temperature include differences in fuel composition and combustion completeness (which can be independent of fire temperature), that the solubility of

some metals changes with pH, and that some metals are likely to be present in complexes with organic matter (which is typically higher in incompletely combusted black ashes; Quill et al., 2010).

In a laboratory study, levoglucosan formed at burn temperatures between 150 and 350°C (Kuo et al., 2008). Kuo et al. (2008) combusted three different wood species (honey mesquite, cordgrass, and loblolly pine), with maximum levoglucosan yield for all species found at 250°C, although large differences in yield were noted between species. Combustion duration had no significant impact on levoglucosan yield from honey mesquite char (Kuo et al., 2008). In the results presented here, levoglucosan is highest in gray and white ashes, noting both the small sample sizes and that the spread of the gray data is high, and that while the highest concentration of levoglucosan was found in a gray ash sample, the lowest non-zero concentration was also found in a gray ash sample. This may indicate that gray ash samples are heterogeneous or comprised of different vegetation types, although to our knowledge no laboratory study has investigated changes in levoglucosan yield from Australian species. Alternatively, the difference between the two gray ash samples may be because levoglucosan production is independent of burn time (Kuo et al., 2008), and the gray sample with a higher levoglucosan concentration may have been produced by long slow smoldering rather than hot fire.

Laboratory and field experiments have shown that low molecular weight PAHs tend to be more abundant in post-fire soils and burn residues after fires at low-to-moderate temperatures (Karp et al., 2020; Kim et al., 2011; Rey-Salgueiro et al., 2018; Simon et al., 2016), with lower concentrations found in laboratory residues at very low (<300°C) and very high (>600°C) temperatures (Karp et al., 2020). In wildfire ashes, summed PAHs have been shown to be higher in black than in white ashes (H. Chen et al., 2018). In the results presented here, PAH concentrations are generally higher in the lower molecular weight PAHs for all ash colors (Figure 7 and Table S10 in Supporting Information S1). Summed PAHs are also generally higher in black and gray ashes (see Figure S4.1 in Text S4 in Supporting Information S1), although there is significant variability in concentrations of the black ash samples (noting that only one each of red and white ashes are presented here). Higher concentrations of PAHs in black and gray ashes is to be expected, as at high temperatures, PAHs may be completely combusted or incorporated into larger aromatic compounds (Karp et al., 2020).

4.1.3. Ash and Soil Leachate Chemistry Varies Among Sites

Ash leachate chemistry varied between sites. Shapley value regression showed that for 16 variables (Ba, Ca, Cl, Co, Cr, Cu, Mg, Na, Sb, Se, Si, SO_4, Sr, total alkalinity, U, and V) location had more influence on ash leachate chemistry than ash color. The second-most important predictor (above the threshold of 0.25, which indicates if a predictor explains more than its share of variance) was the ash color for Ba, Ca, Cl, Co, Cu, Na, Se, Si, SO_4, and total alkalinity. For Cr, years since the last fire was the second-most important predictor, while for Mg, the total number of fires was the second-most important predictor. The importance of location is also shown in the PCA, with ash leachates from different locations clustering differently, with the difference most obvious between the southeast and southwest Australian samples. While there has been limited research on ashes from multiple sites, Úbeda et al. (2009) showed that in laboratory conditions, ash produced from *Quercus suber* from two different sites had distinctly different physical and chemical compositions. Sánchez-García et al. (2023) found that ashes from different sites clustered differently, although they attributed differences between the clusters to delays in sampling post-fire (with samples being rained on, or loss of the finer particles by wind) and to legacy contamination from industrial activity.

To test the potential influence of in situ leaching of the Macleay ashes on the analyses, we repeated the Shapley value regression with those samples removed (see Table S9 in Supporting Information S1). Broadly, results were in good agreement with the analysis of the whole data set, although the importance of location as a predictor variable declined for Cl, Cr, Cu, Na, Se, SO_4, total alkalinity, and V. The greatest reductions in the influence of location were seen for Cl, and Na, which may be expected even without potential in situ leaching, as Macleay samples are less exposed to salt-laden winds than southwest Australian samples. Concentrations of many of the remaining analytes were comparable between southwest and southeast Australia (Figure S6 in Supporting Information S1). That location became less important with the exclusion of the Macleay ash samples is to be expected, as the climate and geology of all sampling sites in southwest Australia are similar. Within the constraints of this data set, it is not possible to determine whether the importance of location as a predictor of ash chemistry is entirely due to in situ leaching of Macleay ash samples. To better determine the impact of location on ash

chemistry, future research should ensure sample collection prior to any precipitation (noting that, as in this instance, this is often not possible to do safely).

Location was the most important predictor for soil leachates, as indicated by the Shapley value regression and PCA results. Sub-plot-scale heterogeneity in soils has been well-documented (J. B. Campbell, 1979; Harris, 1915). The Shapley value regression showed that location was the dominant predictor of all variables. As for ash leachates, a standardized Shapley value >0.25 indicates that a predictor explains more than its share of variance if all predictors had equal predictive power. Unlike for ash leachate results, there are very few variables where the second-most important predictor exceeds this threshold (Cl and V), and for both variables the second-most important predictor was the total number of fires. Both PC1 and PC2 described some aspect of soil sample location, with PC1 perhaps conflating total number of fires and location, while elements which loaded strongly positively on PC2 were related to distance from the coast via sea spray inputs.

4.1.4. Limited Evidence of Memory of Previous Fires in Ash and Soil Leachates

Neither the total number of fires nor the number of years since the last fire (both describing fire history) explained a large proportion of the variance in ash leachate chemistry, although PCA of ash leachates showed that PC2 may describe the number of years since the last fire, with sites which burned more recently loading positively on PC2, and sites which burned less recently loading negatively on PC2. Similarly, sites which had experienced more fires loaded positively on PC2, while sites which had experienced fewer fires loaded negatively on PC2, although the clustering is not as distinct as for the number of years since the last fire. This is reflected in the Shapley value regression, where the number of years since the last fire tends to be a more important predictor than the total number of fires (although less important than either ash color or location). Shapley value regression showed that the number of years since the last fire had a sizable impact on Cr and SO_4 concentrations, while the total number of fires impacted Mg and Ni. This is consistent with Miotliński et al. (2023) who found higher concentrations in ashes produced from leaf litter and soil sampled from a site which had burned recently (2 months) than from a site that had burned less recently (4.5 years). That the effect appears to be tertiary to location and burn severity here may be explained by the much longer interval since the penultimate fire in the results presented here.

As for ash leachates, neither the number of years since the last fire nor the total number of fires explained a large proportion of the variance in soil leachate chemistry, although PC1 may reflect the total number of fires (although this is potentially a confounding effect produced by correlation between location and the total number of fires, with Yanchep recording more fires than sites in the Capes region). Unlike for ash leachates, Shapley value regression of soil leachates suggests that the total number of fires has more impact on soil leachate chemistry than the number of years since the last fire, although only two variables (Cl and V) had standardized Shapley values >0.25.

4.2. Implications for Palaeofire Research

Past fire activity can be reconstructed using inorganic and organic proxies preserved in environmental archives such as soils, sediments, or ice cores. In recent years, speleothems have been used to reconstruct past fire activity in Australia and North America (Argiriadis et al., 2019, 2023; Homann et al., 2022, 2023; McDonough et al., 2022). Fire sensitive stalagmite proxies include trace and minor elements and nutrients, calcite $\delta^{18}O$, and fire-sensitive biomarkers. Trace and minor elements and biomarkers are thought to reach stalagmites after originating in burned vegetation and soil and being carried by infiltrating waters through the vadose zone before being sequestered in the growing stalagmites.

Ash and soil leachates confirm that the inorganic fire signal is likely to originate from the ash, as concentrations of many analytes (including Na, K, Rb, Ba, V, Mn, Co, Ni, Cu, Mo, Si, P, As, Sb, Se, Cl, and SO_4) are generally higher in ash leachates than in soil leachates, although there is some variability by location. Additionally, many elements vary with ash color (itself a proxy for burn severity), suggesting that burn severity as well as fire frequency may be recorded by speleothems, as first suggested by McDonough et al. (2022). While some analytes are both higher in ash leachates than in soil leachates and vary with burn severity (e.g., Na, K, Rb, Mn, P, As, and SO_4) not all may be of sufficient concentration to be detectable by LA-ICP-MS or synchrotron X-ray Fluorescence Microscopy, the standard methods to measure stalagmite trace elements.

The pyrogenic biomarkers analyzed here (six PAHs and levoglucosan) were in low abundance in the majority of ash leachate samples (see Table S10 in Supporting Information S1 for abundances). This may have been due to degradation ex situ when stored at laboratory temperatures (Douglas et al., 2018; Rost et al., 2002). The samples that had measurable biomarkers were collected and analyzed within 2 months, a long enough delay that some degradation can be expected to have occurred (Douglas et al., 2018), although repeat analyses of samples presented here suggest that degradation may be non-linear or secondary to sample heterogeneity (see Figure S4.2 in Text S4 in Supporting Information S1). Douglas et al. (2018) showed that Chrysene and Pyrene were robust to degradation under ambient temperature. Concentrations of both Chrysene and Pyrene in samples presented here were low, and there was no clear trend by ash color for either compound, although in general black and gray ashes had higher concentrations of both compounds. Considering all PAHs presented here, concentrations tended to be higher in the lower molecular weight compounds, and summed concentrations were highest in black and gray ash samples. This is consistent with both laboratory studies and analysis of wildfire ashes, which have demonstrated that the highest PAH concentrations are between 400 and 600°C (Karp et al., 2020) and have shown that total concentrations are higher in black ashes than in white ashes (H. Chen et al., 2018).

Anhydrosugars (including levoglucosan) are reactive and soluble. In open fires, they may appear in all phases (as gas, particles, or in charcoal) (Suciu et al., 2019). Anhydrosugars are released in greatest quantities at ∼300°C (Shafizadeh et al., 1979; Suciu et al., 2019), although a second peak may be observed at 600°C due to the depolymerization of polymeric products formed from the thermal conversion of water-soluble compounds (Suciu et al., 2019, p. 213). Suciu et al. (2019) suggest that it is the reaction of these high-temperature anhydrosugars with aromatic substances which may result in anhydrosugars forming in char. While there is no clear trend in levoglucosan concentration by ash color, in general, concentrations are higher in gray and white ash samples than in black ash samples. As the chemical structure of anhydrosugars means they bond well with chelating metals (e.g., Fe and Al; Suciu et al., 2019), we could have expected that the samples with the highest levoglucosan concentrations would also have high concentrations of Fe and Al. Instead, we find that of those seven samples, the highest concentrations of levoglucosan are found in the sample with the third highest Fe concentrations and the lowest Al concentrations (of the seven Golgotha Cave ash samples presented in Section 3.1.3). As for the PAHs, a larger sample size with reduced opportunity for sample degradation is needed to be able to draw stronger conclusions about the use of levoglucosan as a speleothem palaeofire proxy.

That biomarker concentrations may degrade in both collected samples (Douglas et al., 2018; Rost et al., 2002) and in situ (Kim et al., 2011; Simon et al., 2016; Yang et al., 2010) should be considered when interpreting them as proxies for past fires. For example, in southwest Western Australia, the bushfire season peaks in summer and autumn. Dripwater monitoring at Golgotha Cave has shown that activation of fractures (and so potentially more efficient transport of the surface fire signal) is generally enhanced when soil stores are saturated (Priestley et al., 2023), which may occur months after the fire season has finished. This suggests that where biomarkers are incorporated in speleothems, they may have been degraded prior to inclusion. Additionally, that low molecular weight PAHs are generally more abundant than high molecular weight PAHs, and that total PAH concentrations are higher in black and gray ashes than in white ashes both suggest that PAH-derived records of past fires may be biased toward less-severe burns. Homann et al. (2023) found that high molecular weight PAHs were often <LOD in a Mexican speleothem. They attributed this to filtering of high molecular weight PAHs by overlying soils and epikarsts, as earlier suggested by Perrette et al. (2013). Our results suggest that, if speleothem PAHs are derived from the leaching of deposited ashes, high molecular weight PAHs and PAHs sourced from more severe fires are unlikely to be incorporated, as initial concentrations of both are low, and karst processes are likely to further dilute them. While the results presented here will be useful for the interpretation of pyrogenic biomarkers in speleothems, more research is needed to better understand the transport and deposition of pyrogenic biomarkers in karst systems.

4.3. Implications for Surface and Groundwaters

The impact of wildfires on surface waters has been well-documented, and elevated concentrations of contaminants are commonly seen (Beyene et al., 2023; Hickenbottom et al., 2023), along with increased turbidity (J. Chen & Chang, 2023; Emmerton et al., 2020) and changes in pH (Costa et al., 2014; Granath et al., 2021), all of which pose a risk to both natural and human systems. Karst systems make up 7%–12% of the terrestrial earth surface, and ∼25% of the world's population rely on karst aquifers for their water supply (Ford & Williams, 2007; Hartmann et al., 2014). While groundwaters are generally thought to be less susceptible to contamination than

surface waters (Reberski et al., 2022), contamination of karst groundwaters is a known concern (Vilhar et al., 2022). Contaminants may be both autogenic and allogenic, occurring as both point-source and diffuse sources (Ford & Williams, 2007). Karst aquifers are susceptible to pollution because they transport contaminants efficiently and have limited capacity to filter them (Ford & Williams, 2007; Sasowsky, 2000). Karst aquifers have been contaminated by a range of pollutants such as fertilizers, pesticides, pharmaceuticals, microplastics, effluent, and urban and agricultural runoff (Jiménez-Sánchez et al., 2008; Panno et al., 2019; Reberski et al., 2022). That karst aquifers may be more susceptible to contamination than non-karst aquifers is demonstrated by Reberski et al. (2022), who in a review of 50 studies of anthropogenic contaminants in karst aquifers showed that while concentrations of anthropogenic contaminants were lower in karst aquifers than in surface waters, karst aquifers had higher concentrations of those contaminants than other aquifers.

There has been limited research on the impact of fire as a contaminant source in karst aquifers, but land clearing and fire are both thought to result in heightened nutrient loading in karst systems (Gillieson & Thurgate, 1999). In the karst vadose zone, the geochemical response to fires in dripwater is variable, and appears to depend on both the burn severity and the cave depth (Coleborn et al., 2018, 2019; Nagra et al., 2016; Treble et al., 2016). Fires have also been implicated in enhanced recharge in the vadose zone through heat-induced fracturing of the host rock (McDonough et al., 2022; Meng et al., 2020; Wu & Wang, 2012). McDonough et al. (2022) attributed enhanced organic matter in a speleothem to increased fracture flow following a severe bushfire. Fires have also been implicated in reduced infiltration in karst due to sealing of the epikarst (the uppermost layer of the karst; Holland, 1994), although there has been little reporting of this effect. Metals are listed as a key karst contaminant (Vesper et al., 2003), and the results presented here show that post-fire ashes may be a point-source of metal contamination at concentrations higher than normally found in soils. Concentrations of key potential contaminants (As, Ba, Co, Cu, Mn, Mo, Ni, Sn, V, Zn, P, S, SO_4, Phenanthrene, Anthracene, Pyrene, and Benzopyrene) in both ash and soil leachates are generally lower than the Western Australian Ecological Investigation Levels (Department of Environment and Conservation, 2010; see Table S14 in Supporting Information S1), with the exception of S and SO_4, which both exceed the ecological investigation levels. While concentrations are generally low, ash leachate concentrations are much higher than soil leachate concentrations (Table S14 in Supporting Information S1). It is unclear how pulses of these potential contaminants might impact the karst environment, including both fragile cave ecosystems and water resources. Further investigation is required at scales ranging from the cave to the catchment to determine whether ash inputs are a significant contamination source for karst aquifers. Since climate change is likely to strain global water resources, and since karst aquifers make such a large contribution to global water resources, understanding how best to minimize their contamination is needed to ensure future water security.

5. Conclusion

Ashes from both wild and prescribed fires are sources of both contaminants and potential fire proxies for palaeoenvironmental research. In our analyses of ash leachates from ashes collected in both southwest and southeast Australia, we found that ash leachate inorganic chemistry primarily varies with ash color (which is an indicator of burn severity) and location. Statistical difference in inorganic analyte concentration by ash color was mainly found between the ash color severity "end-members" (i.e., black vs. white ashes). This suggests that palaeoenvironmental applications of the relationships between inorganic ash chemistry and burn severity will likely be limited to being able to differentiate between more and less severe burns.

PCA and Shapley value regression demonstrated that location and, to a lesser extent, fire history also influence inorganic ash leachate chemistry. The PCA demonstrated that while the first PC explained ash color, the second PC explained location, with samples from southeast Australia clustering differently to samples from southwest Australia. Shapley value regression found that location was the dominant predictor of ash inorganic chemistry, although ash color was generally the second-most important predictor. It should be noted that the collection of samples from southeast Australia was delayed, and so the time the ashes spent degrading and reacting in the environment may be more important than location, as suggested elsewhere (Sánchez-García et al., 2023). Fire histories, including the number of years since the last fire, and the total number of fires on record for each collection point, had limited influence on ash leachate inorganic chemistry. This is a positive outcome for palaeoenvironmental applications, as we can assume that there is little memory in the system as fire history was generally a poor predictor of ash and soil chemistry, and the chemistry of ash produced by each fire event should

largely be independent of past fires. This means that relative fire severities at a site should be able to be determined after consideration of any vegetation or land use changes.

The relationship between ash leachate inorganic chemistry and elemental volatilization temperature did not wholly account for the differences in ash leachates by ash color. Competing factors which may explain why some analytes are higher in less combusted ashes than in more combusted ashes (or vice versa) include fuel composition, that combustion completeness may be independent of burn temperature, that pH affects the solubility of many elements, that some metals will form complexes with organic matter, and that some ashes potentially degraded prior to sampling (i.e., potential removal of fine grains and dissolved elements).

A comparison of ash leachate results presented here with a those published elsewhere showed significant heterogeneity in ash leachate inorganic geochemistry, including in how geochemistry differed between black and white ashes. This suggests some level of site or regional specificity, which is an important consideration for any palaeofire reconstruction. We note that our results showed good agreement with Miotliński et al. (2023), the only other analysis of ash leachates from southwest Australia. For most elements, concentrations were higher in ash leachates than in soil leachates. Soil chemistry was largely controlled by location, and sample depth had minimal impact. This may be attributed to sandy well-drained soils or to the coarse sampling resolution. The fact that elemental concentrations are generally higher in ashes than in soils is important for speleothem palaeofire research, as it suggests that the signal is sourced from ash, and not from soil, as seen elsewhere (Hartland et al., 2012). Elements which are higher in soil leachates than in ash leachates (e.g., Fe) may be the key to fingerprinting soil geochemical inputs. Key analytes which should be considered in future speleothem palaeofire research include Na, K, Rb, Mn, P, As, Se, V, Cl, and SO_4, as these analytes all varied significantly in leachates of black and white ashes, and are all readily measured in calcite via LA-ICP-MS or SIMS (with sulfate measured as elemental S), and are all generally of higher concentrations in ash leachates than in soil leachates. The results presented here will inform future speleothem palaeofire research although additional complexities such as karst processes and differing partition coefficients between cave waters and calcite must be considered. Care must also be taken in the selection of appropriate samples (M. Campbell et al., 2023).

The preliminary biomarker results presented here were inconclusive, although PAH concentrations were generally higher in black ash samples than in white ash samples, and levoglucosan concentrations were generally higher in gray and white samples than in black samples. While degradation ex situ may account for some inconsistency, further analyses are needed to establish the potential relationships between these biomarkers and burn severity, how these biomarkers degrade in nature, and the implications of for speleothem palaeofire research.

Data Availability Statement

Data and scripts for the statistical analyses and data visualization are available at https://doi.org/10.6084/m9.figshare.25001858 (M. Campbell et al., 2024). These data are published under a CC BY 4.0 License.

Acknowledgments
This research was funded by the Australian Government through the Australian Research Council (project number DP200100203). MC was also supported by an Early Career Research Grant from the Australian Institute of Nuclear Science and Engineering. We thank Yanchep National Parks staff, Calgardup Caves staff, the Kempsey Speleological Society, and Lachie MacCaw for assistance with sample collection. Thanks to Brett Rowling and Chris Vardanega at ANSTO ITNS for analyses of ash leachates. Thanks to Eve Slavich from UNSW Stats Central for statistical advice, and to Morgan Williams for productive conversation on the analysis of compositional data. We also thank Cameron Ritchie for helpful pointers on the geology of southwest WA and Tim Payne for discussion of leachate chemistry. Thank you to the two anonymous reviewers for their thoughtful comments, and to Dr. Branwen Williams for handling the manuscript. We respectfully acknowledge the Whadjuk Noongar, Wadandi Noongar, and Dunghutti peoples as the traditional and spiritual custodians of the Yanchep (on Whadjuk Noongar boodja), Margaret River (on Wadandi boodja), and Macleay regions (on Dunghutti lands), where samples were collected for this research. Open access publishing facilitated by University of New South Wales, as part of the Wiley - University of New South Wales agreement via the Council of Australian University Librarians.

References

American Public Health Association, American Water Works Association, Water Environment Federation, R. B. Baird, A. D. Eaton, & E. W. Rice (Eds.). (2017). *Standard methods for the examination of water and wastewater* (23rd ed.). APHA Press.

Argiriadis, E., Denniston, R. F., & Barbante, C. (2019). Improved polycyclic aromatic hydrocarbon and n-alkane determination in speleothems through cleanroom sample processing. *Analytical Chemistry*, *91*(11), 7007–7011. https://doi.org/10.1021/acs.analchem.9b00767

Argiriadis, E., Denniston, R. F., Ondei, S., Bowman, D. M. J. S., Genuzio, G., Nguyen, H. Q. A., et al. (2023). Polycyclic aromatic hydrocarbons in tropical Australian stalagmites: A framework for reconstructing paleofire activity. *Geochimica et Cosmochimica Acta*, *366*, 250–266. https://doi.org/10.1016/j.gca.2023.11.033

Bai, J., Sun, X., Zhang, C., Xu, Y., & Qi, C. (2013). The OH-initiated atmospheric reaction mechanism and kinetics for levoglucosan emitted in biomass burning. *Chemosphere*, *93*(9), 2004–2010. https://doi.org/10.1016/j.chemosphere.2013.07.021

Baker, A., Berthelin, R., Cuthbert, M. O., Treble, P. C., Hartmann, A., & KSS Cave Studies Team, T. (2020). Rainfall recharge thresholds in a subtropical climate determined using a regional cave drip water monitoring network. *Journal of Hydrology*, *587*, 125001. https://doi.org/10.1016/j.jhydrol.2020.125001

Balfour, V. N., & Woods, S. W. (2013). The hydrological properties and the effects of hydration on vegetative ash from the Northern Rockies, USA. *Catena*, *111*, 9–24. https://doi.org/10.1016/j.catena.2013.06.014

Beyene, M. T., Leibowitz, S. G., Dunn, C. J., & Bladon, K. D. (2023). To burn or not to burn: An empirical assessment of the impacts of wildfires and prescribed fires on trace element concentrations in Western US streams. *Science of the Total Environment*, *863*, 160731. https://doi.org/10.1016/j.scitotenv.2022.160731

Bhattarai, H., Saikawa, E., Wan, X., Zhu, H., Ram, K., Gao, S., et al. (2019). Levoglucosan as a tracer of biomass burning: Recent progress and perspectives. *Atmospheric Research*, *220*, 20–33. https://doi.org/10.1016/j.atmosres.2019.01.004

Bivand, R., Keitt, T., & Rowlingson, B. (2021). rgdal: Bindings for the "geospatial" data abstraction library [Software]. *CRAN*. Retrieved from https://cran.r-project.org/web/packages/rgdal/index.html

Blumenstock, M., Zimmermann, R., Schramm, K.-W., & Kettrup, A. (2000). Influence of combustion conditions on the PCDD/F-PCB-PCBz- and PAH-concentrations in the post-combustion chamber of a waste incineration pilot plant. *Chemosphere*, *40*(9–11), 987–993. https://doi.org/10.1016/S0045-6535(99)00343-4

Bodí, M. B., Martin, D. A., Balfour, V. N., Santín, C., Doerr, S. H., Pereira, P., et al. (2014). Wildland fire ash: Production, composition and eco-hydro-geomorphic effects. *Earth-Science Reviews*, *130*, 103–127. https://doi.org/10.1016/j.earscirev.2013.12.007

Budescu, D. V. (1993). Dominance analysis: A new approach to the problem of relative importance of predictors in multiple regression. *Psychological Bulletin*, *114*(3), 542–551. https://doi.org/10.1037/0033-2909.114.3.542

Burton, C. A., Hoefen, T. M., Plumlee, G. S., Baumberger, K. L., Backlin, A. R., Gallegos, E., & Fisher, R. N. (2016). Trace elements in stormflow, ash, and burned soil following the 2009 station fire in southern California. *PLoS One*, *11*(5), e0153372. https://doi.org/10.1371/journal.pone.0153372

Campbell, J. B. (1979). Spatial variability of soils. *Annals of the Association of American Geographers*, *69*(4), 544–556. https://doi.org/10.1111/j.1467-8306.1979.tb01281.x

Campbell, M., McDonough, L., Treble, P. C., Baker, A., Kosarac, N., Coleborn, K., et al. (2023). A review of speleothems as archives for paleofire proxies, with Australian case studies. *Reviews of Geophysics*, *61*(2), e2022RG000790. https://doi.org/10.1029/2022RG000790

Campbell, M., Treble, P. C., McDonough, L. K., Naeher, S., Baker, A., Grierson, P. F., et al. (2024). Australian ash and soil leachate data and scripts supporting the article "Combustion completeness and sample location determine wildfire ash leachate chemistry" [Dataset]. *Figshare*. https://doi.org/10.6084/m9.figshare.25001858

Canty, A., & Ripley, B. D. (2022). boot: Bootstrap R (S-plus) functions [Software]. *CRAN*. Retrieved from https://cran.r-project.org/web/packages/boot/index.html

Carpenter, J., & Bithell, J. (2000). Bootstrap confidence intervals: When, which, what? A practical guide for medical statisticians. *Statistics in Medicine*, *19*(9), 1141–1164. https://doi.org/10.1002/(SICI)1097-0258(20000515)19:9<1141::AID-SIM479>3.0.CO;2-F

Certini, G. (2005). Effects of fire on properties of forest soils: A review. *Oecologia*, *143*, 1–10. https://doi.org/10.1007/s00442-004-1788-8

Chapin, F. S., Matson, P. A., & Vitousek, P. M. (2011). *Principles of terrestrial ecosystem ecology*. Springer. https://doi.org/10.1007/978-1-4419-9504-9

Chen, H., Chow, A. T., Li, X.-W., Ni, H.-G., Dahlgren, R. A., Zeng, H., & Wang, J.-J. (2018). Wildfire burn intensity affects the quantity and speciation of polycyclic aromatic hydrocarbons in soils. *ACS Earth and Space Chemistry*, *2*(12), 1262–1270. https://doi.org/10.1021/acsearthspacechem.8b00101

Chen, J., & Chang, H. (2023). A review of wildfire impacts on stream temperature and turbidity across scales. *Progress in Physical Geography: Earth and Environment*, *47*(3), 369–394. https://doi.org/10.1177/03091333221118363

Cheng, H., Edwards, R. L., Sinha, A., Spötl, C., Yi, L., Chen, S., et al. (2016). The Asian monsoon over the past 640,000 years and ice age terminations. *Nature*, *534*(7609), 640–646. https://doi.org/10.1038/nature18591

Coleborn, K., Baker, A., Treble, P. C., Andersen, M. S., Baker, A., Tadros, C. V., et al. (2018). The impact of fire on the geochemistry of speleothem-forming drip water in a sub-alpine cave. *Science of the Total Environment*, *642*, 408–420. https://doi.org/10.1016/j.scitotenv.2018.05.310

Coleborn, K., Baker, A., Treble, P. C., Andersen, M. S., Baker, A., Tadros, C. V., et al. (2019). Corrigendum to "The impact of fire on the geochemistry of speleothem-forming drip water in a sub-alpine cave" [Sci. Total Environ. (2018) 408–420]. *Science of the Total Environment*, *668*, 1339–1340. https://doi.org/10.1016/j.scitotenv.2019.02.350

Costa, M. R., Calvão, A. R., & Aranha, J. (2014). Linking wildfire effects on soil and water chemistry of the Marão River watershed, Portugal, and biomass changes detected from Landsat imagery. *Applied Geochemistry*, *44*, 93–102. https://doi.org/10.1016/j.apgeochem.2013.09.009

Croke, J., Vítkovský, J., Hughes, K., Campbell, M., Amirnezhad-Mozhdehi, S., Parnell, A., et al. (2021). A palaeoclimate proxy database for water security planning in Queensland Australia. *Scientific Data*, *8*(1), 292. https://doi.org/10.1038/s41597-021-01074-8

Dasgupta, S., Siegel, D. I., Zhu, C., Chanton, J. P., & Glaser, P. H. (2015). Geochemical mixing in peatland waters: The role of organic acids. *Wetlands*, *35*(3), 567–575. https://doi.org/10.1007/s13157-015-0646-2

Davies, P. J., & Crosbie, R. S. (2018). Mapping the spatial distribution of chloride deposition across Australia. *Journal of Hydrology*, *561*, 76–88. https://doi.org/10.1016/j.jhydrol.2018.03.051

Davison, A. C., & Hinkley, D. V. (1997). Bootstrap methods and their applications. Cambridge University Press.

Denis, E. H., Toney, J. L., Tarozo, R., Scott Anderson, R., Roach, L. D., & Huang, Y. (2012). Polycyclic aromatic hydrocarbons (PAHs) in lake sediments record historic fire events: Validation using HPLC-fluorescence detection. *Organic Geochemistry*, *45*, 7–17. https://doi.org/10.1016/j.orggeochem.2012.01.005

Department of Environment and Conservation. (2010). *Assessment levels for soil, sediment and water, contaminated sites management Series*. Government of Western Australia.

Dixon, D. J., Callow, J. N., Duncan, J. M. A., Setterfield, S. A., & Pauli, N. (2022). Regional-scale fire severity mapping of Eucalyptus forests with the Landsat archive. *Remote Sensing of Environment*, *270*, 112863. https://doi.org/10.1016/j.rse.2021.112863

Domínguez-Villar, D., Fairchild, I. J., Baker, A., Wang, X., Edwards, R. L., & Cheng, H. (2009). Oxygen isotope precipitation anomaly in the North Atlantic region during the 8.2 ka event. *Geology*, *37*(12), 1095–1098. https://doi.org/10.1130/G30393A.1

Douglas, G., Hardenstine, J., Rouhani, S., Kong, D., Arnold, R., & Gala, W. (2018). Chemical preservation of semi-volatile polycyclic aromatic hydrocarbon compounds at ambient temperature: A sediment sample holding time study. *Archives of Environmental Contamination and Toxicology*, *75*(3), 486–494. https://doi.org/10.1007/s00244-018-0517-y

Dunn, O. J. (1964). Multiple comparisons using rank sums. *Technometrics*, *6*(3), 241–252. https://doi.org/10.2307/1266041

Elias, V. O., Simoneit, B. R. T., Cordeiro, R. C., & Turcq, B. (2001). Evaluating levoglucosan as an indicator of biomass burning in Carajás, amazônia: A comparison to the charcoal record 22 associate editor: R. Summons. *Geochimica et Cosmochimica Acta*, *65*(2), 267–272. https://doi.org/10.1016/S0016-7037(00)00522-6

Emmerton, C. A., Cooke, C. A., Hustins, S., Silins, U., Emelko, M. B., Lewis, T., et al. (2020). Severe western Canadian wildfire affects water quality even at large basin scales. *Water Research*, *183*, 116071. https://doi.org/10.1016/j.watres.2020.116071

Fontaine, J. (2022). *Yanchep bushfire analysis—Black Summer final report*. Bushfire and Natural Hazards CRC.

Ford, D., & Williams, P. (2007). *Karst hydrogeology and geomorphology* (1st ed.). Wiley. https://doi.org/10.1002/9781118684986

Gabet, E. J., & Bookter, A. (2011). Physical, chemical and hydrological properties of Ponderosa pine ash. *International Journal of Wildland Fire*, *20*(3), 443–452. https://doi.org/10.1071/WF09105

Geoscience Australia. (2006). GEODATA TOPO 250K Series 3—(Personal geodatabase format) [Dataset]. *Geoscience Australia, Canberra*. Retrieved from http://pid.geoscience.gov.au/dataset/ga/63999

Giglio, L., van der Werf, G. R., Randerson, J. T., Collatz, G. J., & Kasibhatla, P. (2006). Global estimation of burned area using MODIS active fire observations. *Atmospheric Chemistry and Physics*, *6*(4), 957–974. https://doi.org/10.5194/acp-6-957-2006

Gillieson, D., & Thurgate, M. (1999). Karst and agriculture in Australia. *International Journal of Speleology*, *28*(1), 149–168. https://doi.org/10.5038/1827-806X.28.1.11

Granath, G., Evans, C. D., Strengbom, J., Fölster, J., Grelle, A., Strömqvist, J., & Köhler, S. J. (2021). The impact of wildfire on biogeochemical fluxes and water quality in boreal catchments. *Biogeosciences*, *18*(10), 3243–3261. https://doi.org/10.5194/bg-18-3243-2021

Hageman, P. L. (2007). U.S. Geological Survey field leach test for assessing water reactivity and leaching potential of mine wastes, soils, and other geologic and environmental materials (USGS numbered Series No. 5-D3), U.S. Geological Survey field leach test for assessing water reactivity and leaching potential of mine wastes, soils, and other geologic and environmental materials. *Techniques and Methods*. https://doi.org/10.3133/tm5D3

Harris, J. A. (1915). On a criterion of substratum homogeneity (or heterogeneity) in field experiments. *The American Naturalist*, *49*(583), 430–454. https://doi.org/10.1086/279492

Hartland, A., Fairchild, I. J., Lead, J. R., Borsato, A., Baker, A., Frisia, S., & Baalousha, M. (2012). From soil to cave: Transport of trace metals by natural organic matter in karst dripwaters. *Chemical Geology*, *304–305*, 68–82. https://doi.org/10.1016/j.chemgeo.2012.01.032

Hartmann, A., Goldscheider, N., Wagener, T., Lange, J., & Weiler, M. (2014). Karst water resources in a changing world: Review of hydrological modeling approaches. *Reviews of Geophysics*, *52*(3), 218–242. https://doi.org/10.1002/2013RG000443

Hickenbottom, K., Pagilla, K., & Hanigan, D. (2023). Wildfire impact on disinfection byproduct precursor loading in mountain streams and rivers. *Water Research*, *244*, 120474. https://doi.org/10.1016/j.watres.2023.120474

Hogue, B. A., & Inglett, P. W. (2012). Nutrient release from combustion residues of two contrasting herbaceous vegetation types. *Science of the Total Environment*, *431*, 9–19. https://doi.org/10.1016/j.scitotenv.2012.04.074

Holland, E. (1994). The effects of fire on soluble rock landscapes. *Helictite*, *32*, 3–10.

Hollander, M., & Wolfe, D. A. (1973). *Nonparametric statistical methods*. John Wiley & Sons.

Homann, J., Karbach, N., Carolin, S. A., James, D. H., Hodell, D., Breitenbach, S. F. M., et al. (2023). Past fire dynamics inferred from polycyclic aromatic hydrocarbons and monosaccharide anhydrides in a stalagmite from the archaeological site of Mayapan, Mexico. *Biogeosciences*, *20*(15), 3249–3260. https://doi.org/10.5194/bg-20-3249-2023

Homann, J., Oster, J. L., de Wet, C. B., Breitenbach, S. F. M., & Hoffmann, T. (2022). Linked fire activity and climate whiplash in California during the early Holocene. *Nature Communications*, *13*, 1–9. https://doi.org/10.1038/s41467-022-34950-x

Jiménez-Sánchez, M., Stoll, H., Vadillo, I., López-Chicano, M., Domínguez-Cuesta, M., Martín-Rosales, W., & Meléndez-Asensio, M. (2008). Groundwater contamination in caves: Four case studies in Spain. *International Journal of Speleology*, *37*(1), 53–66. https://doi.org/10.5038/1827-806X.37.1.5

Johansson, I., & van Bavel, B. (2003). Levels and patterns of polycyclic aromatic hydrocarbons in incineration ashes. *Science of the Total Environment*, *311*(1–3), 221–231. https://doi.org/10.1016/S0048-9697(03)00168-2

Jones, M. W., Abatzoglou, J. T., Veraverbeke, S., Andela, N., Lasslop, G., Forkel, M., et al. (2022). Global and regional trends and drivers of fire under climate change. *Reviews of Geophysics*, *60*(3), e2020RG000726. https://doi.org/10.1029/2020RG000726

Karp, A. T., Holman, A. I., Hopper, P., Grice, K., & Freeman, K. H. (2020). Fire distinguishers: Refined interpretations of polycyclic aromatic hydrocarbons for paleo-applications. *Geochimica et Cosmochimica Acta*, *289*, 93–113. https://doi.org/10.1016/j.gca.2020.08.024

Key, C. H., & Benson, N. C. (2006). Landscape Assessment (LA) (No. 164), IREMON: Fire effects monitoring and inventory system.

Khanna, P. K., Raison, R. J., & Falkiner, R. A. (1994). Chemical properties of ash derived from Eucalyptus litter and its effects on forest soils. *Forest Ecology and Management, Ameliorative Practices for Restoring and Maintaining*, *66*(1–3), 107–125. https://doi.org/10.1016/0378-1127(94)90151-1

Kim, E. J., Choi, S.-D., & Chang, Y.-S. (2011). Levels and patterns of polycyclic aromatic hydrocarbons (PAHs) in soils after forest fires in South Korea. *Environmental Science & Pollution Research*, *18*(9), 1508–1517. https://doi.org/10.1007/s11356-011-0515-3

Kuo, L.-J., Herbert, B. E., & Louchouarn, P. (2008). Can levoglucosan be used to characterize and quantify char/charcoal black carbon in environmental media? *Organic Geochemistry*, *39*(10), 1466–1478. https://doi.org/10.1016/j.orggeochem.2008.04.026

Li, Y., Fu, T.-M., Yu, J. Z., Feng, X., Zhang, L., Chen, J., et al. (2021). Impacts of chemical degradation on the global budget of atmospheric levoglucosan and its use as a biomass burning tracer. *Environmental Science & Technology*, *55*(8), 5525–5536. https://doi.org/10.1021/acs.est.0c07313

Liang, J. (2021). ShapleyValue: Shapley value regression for relative importance of attributes [Software]. *CRAN*. Retrieved from https://cran.r-project.org/web/packages/ShapleyValue/index.html

Lipovetsky, S., & Conklin, M. (2001). Analysis of regression in game theory approach. *Applied Stochastic Models in Business and Industry*, *17*(4), 319–330. https://doi.org/10.1002/asmb.446

Lizundia-Loiola, J., Otón, G., Ramo, R., & Chuvieco, E. (2020). A spatio-temporal active-fire clustering approach for global burned area mapping at 250 m from MODIS data. *Remote Sensing of Environment*, *236*, 111493. https://doi.org/10.1016/j.rse.2019.111493

Marion, G. M., Moreno, J. M., & Oechel, W. C. (1991). Fire severity, ash deposition, and clipping effects on soil nutrients in chaparral. *Soil Science Society of America Journal*, *55*(1), 235–240. https://doi.org/10.2136/sssaj1991.03615995005500010040x

Marlon, J. R., Bartlein, P. J., Carcaillet, C., Gavin, D. G., Harrison, S. P., Higuera, P. E., et al. (2008). Climate and human influences on global biomass burning over the past two millennia. *Nature Geoscience*, *1*(10), 697–702. https://doi.org/10.1038/ngeo313

McDonough, L. K., Treble, P. C., Baker, A., Borsato, A., Frisia, S., Nagra, G., et al. (2022). Past fires and post-fire impacts reconstructed from a southwest Australian stalagmite. *Geochimica et Cosmochimica Acta*, *325*, 258–277. https://doi.org/10.1016/j.gca.2022.03.020

Meng, Q.-B., Wang, C.-K., Liu, J.-F., Zhang, M.-W., Lu, M.-M., & Wu, Y. (2020). Physical and micro-structural characteristics of limestone after high temperature exposure. *Bulletin of Engineering Geology and the Environment*, *79*(3), 1259–1274. https://doi.org/10.1007/s10064-019-01620-0

Millard, S. P. (2013). EnvStats: An R package for environmental statistics [Software]. *Springer*. Retrieved from https://link.springer.com/book/10.1007/978-1-4614-8456-1

Miotliński, K., Tshering, K., Boyce, M. C., Blake, D., & Horwitz, P. (2023). Simulated temperatures of forest fires affect water solubility in soil and litter. *Ecological Indicators*, *150*, 110236. https://doi.org/10.1016/j.ecolind.2023.110236

Misra, M. K., Ragland, K. W., & Baker, A. J. (1993). Wood ash composition as a function of furnace temperature. *Biomass and Bioenergy, Biomass in Combustion: The Challenge of Biomass*, *4*(2), 103–116. https://doi.org/10.1016/0961-9534(93)90032-Y

Nagra, G., Treble, P. C., Andersen, M. S., Fairchild, I. J., Coleborn, K., & Baker, A. (2016). A post-wildfire response in cave dripwater chemistry. *Hydrology and Earth System Sciences*, *20*(7), 2745–2758. https://doi.org/10.5194/hess-20-2745-2016

NSW Department of Environment, Climate Change, and Water. (2011). Guide to New South Wales karst and caves.

NSW Rural Fire Service. (2020). Spring fires torment northern NSW. In *Bush Fire Bulletin* (Vol. 42, pp. 8–9).

Otto, A., Gondokusumo, R., & Simpson, M. J. (2006). Characterization and quantification of biomarkers from biomass burning at a recent wildfire site in Northern Alberta, Canada. *Applied Geochemistry*, *21*(1), 166–183. https://doi.org/10.1016/j.apgeochem.2005.09.007

Panno, S. V., Kelly, W. R., Scott, J., Zheng, W., McNeish, R. E., Holm, N., et al. (2019). Microplastic contamination in karst groundwater systems. *Groundwater*, *57*(2), 189–196. https://doi.org/10.1111/gwat.12862

Pebesma, E. (2018). Simple features for R: Standardized support for spatial vector data. *The R Journal*, *10*(1), 439–446. https://doi.org/10.32614/RJ-2018-009

Pereira, P., & Úbeda, X. (2010). Spatial distribution of heavy metals released from ashes after a wildfire. *Journal of Environmental Engineering and Landscape Management*, *18*(1), 13–22. https://doi.org/10.3846/jeelm.2010.02

Pereira, P., Úbeda, X., & Martin, D. A. (2012). Fire severity effects on ash chemical composition and water-extractable elements. *Geoderma, Fire Effects on Soil Properties*, *191*, 105–114. https://doi.org/10.1016/j.geoderma.2012.02.005

Perrette, Y., Poulenard, J., Durand, A., Quiers, M., Malet, E., Fanget, B., & Naffrechoux, E. (2013). Atmospheric sources and soil filtering of PAH content in karst seepage waters. *Organic Geochemistry*, *65*, 37–45. https://doi.org/10.1016/j.orggeochem.2013.10.005

Perrette, Y., Poulenard, J., Saber, A.-I., Fanget, B., Guittonneau, S., Ghaleb, B., & Garaudee, S. (2008). Polycyclic Aromatic Hydrocarbons in stalagmites: Occurrence and use for analyzing past environments. *Chemical Geology*, *251*(1–4), 67–76. https://doi.org/10.1016/j.chemgeo.2008.02.013

Playford, P. E., Cockbain, A. E., & Low, G. H. (1976). *Geology of the Perth basin Western Australia (bulletin no. 124)*. Geological Survey of Western Australia.

Priestley, S. C., Treble, P. C., Griffiths, A. D., Baker, A., Abram, N. J., & Meredith, K. T. (2023). Caves demonstrate decrease in rainfall recharge of southwest Australian groundwater is unprecedented for the last 800 years. *Communications Earth & Environment*, *4*, 1–12. https://doi.org/10.1038/s43247-023-00858-7

Puth, M.-T., Neuhäuser, M., & Ruxton, G. D. (2015). On the variety of methods for calculating confidence intervals by bootstrapping. *Journal of Animal Ecology*, *84*(4), 892–897. https://doi.org/10.1111/1365-2656.12382

QGIS Development Team. (2022). QGIS geographic information system, version 3.28 [Software]. *QGIS Association*. Retrieved from https://www.qgis.org/en/site/

Qian, Y., Miao, S. L., Gu, B., & Li, Y. C. (2009). Effects of burn temperature on ash nutrient forms and availability from Cattail (Typha domingensis) and Sawgrass (Cladium jamaicense) in the Florida Everglades. *Journal of Environmental Quality*, *38*(2), 451–464. https://doi.org/10.2134/jeq2008.0126

Quill, E. S., Angove, M. J., Morton, D. W., & Johnson, B. B. (2010). Characterisation of dissolved organic matter in water extracts of thermally altered plant species found in boxironbark forests. *Australian Journal of Soil Research*, *48*(8), 693–704. https://doi.org/10.1071/SR09157

Quintana, J. R., Cala, V., Moreno, A. M., & Parra, J. G. (2007). Effect of heating on mineral components of the soil organic horizon from a Spanish juniper (Juniperus thurifera L.) woodland. *Journal of Arid Environments*, *71*(1), 45–56. https://doi.org/10.1016/j.jaridenv.2007.03.002

R Core Team. (2023). R: A language and environment for statistical computing [Software]. *R Foundation for Statistical Computing, Vienna, Austria*. Retrieved from https://www.r-project.org/

Reberski, J., Terzić, J., Maurice, L. D., & Lapworth, D. J. (2022). Emerging organic contaminants in karst groundwater: A global level assessment. *Journal of Hydrology*, *604*, 127242. https://doi.org/10.1016/j.jhydrol.2021.127242

Rehn, E., Rowe, C., Ulm, S., Woodward, C., & Bird, M. (2021). A late-Holocene multiproxy fire record from a tropical savanna, eastern Arnhem Land, Northern Territory, Australia. *The Holocene*, *31*(5), 870–883. https://doi.org/10.1177/0959683620988030

Rey-Salgueiro, L., Martínez-Carballo, E., Merino, A., Vega, J. A., Fonturbel, M. T., & Simal-Gandara, J. (2018). Polycyclic aromatic hydrocarbons in soil organic horizons depending on the soil burn severity and type of ecosystem. *Land Degradation & Development*, *29*(7), 2112–2123. https://doi.org/10.1002/ldr.2806

Rosner, B. (1983). Percentage points for a generalized ESD many-outlier procedure. *Technometrics*, *25*(2), 165–172. https://doi.org/10.1080/00401706.1983.10487848

Rost, H., Loibner, A. P., Hasinger, M., Braun, R., & Szolar, O. H. J. (2002). Behavior of PAHs during cold storage of historically contaminated soil samples. *Chemosphere*, *49*(10), 1239–1246. https://doi.org/10.1016/S0045-6535(02)00497-6

Roy, D. P., Boschetti, L., Maier, S. W., & Smith, A. M. S. (2010). Field estimation of ash and char colour-lightness using a standard grey scale. *International Journal of Wildland Fire*, *19*(6), 698. https://doi.org/10.1071/WF09133

Rubino, M., D'Onofrio, A., Seki, O., & Bendle, J. A. (2016). Ice-core records of biomass burning. *The Anthropocene Review*, *3*(2), 140–162. https://doi.org/10.1177/2053019615605117

Sánchez-García, C., Santín, C., Neris, J., Sigmund, G., Otero, X. L., Manley, J., et al. (2023). Chemical characteristics of wildfire ash across the globe and their environmental and socio-economic implications. *Environment International*, *178*, 108065. https://doi.org/10.1016/j.envint.2023.108065

Santín, C., Doerr, S. H., Otero, X. L., & Chafer, C. J. (2015). Quantity, composition and water contamination potential of ash produced under different wildfire severities. *Environmental Research*, *142*, 297–308. https://doi.org/10.1016/j.envres.2015.06.041

Sasowsky, I. D. (Ed.). (2000). *Groundwater flow and contaminant transport in carbonate aquifers*. Balkema.

Shafizadeh, F., Furneaux, R. H., Cochran, T. G., Scholl, J. P., & Sakai, Y. (1979). Production of levoglucosan and glucose from pyrolysis of cellulosic materials. *Journal of Applied Polymer Science*, *23*(12), 3525–3539. https://doi.org/10.1002/app.1979.070231209

Simon, E., Choi, S.-D., & Park, M.-K. (2016). Understanding the fate of polycyclic aromatic hydrocarbons at a forest fire site using a conceptual model based on field monitoring. *Journal of Hazardous Materials*, *317*, 632–639. https://doi.org/10.1016/j.jhazmat.2016.06.030

Simoneit, B. R. T., Schauer, J. J., Nolte, C. G., Oros, D. R., Elias, V. O., Fraser, M. P., et al. (1999). Levoglucosan, a tracer for cellulose in biomass burning and atmospheric particles. *Atmospheric Environment*, *33*(2), 173–182. https://doi.org/10.1016/S1352-2310(98)00145-9

Stronach, N. R. H., & McNaughton, S. J. (1989). Grassland fire dynamics in the serengeti ecosystem, and a potential method of retrospectively estimating fire energy. *Journal of Applied Ecology*, *26*(3), 1025–1033. https://doi.org/10.2307/2403709

Suciu, L. G., Masiello, C. A., & Griffin, R. J. (2019). Anhydrosugars as tracers in the Earth system. *Biogeochemistry*, *146*(3), 209–256. https://doi.org/10.1007/s10533-019-00622-0

Treble, P. C., Fairchild, I. J., Baker, A., Meredith, K. T., Andersen, M. S., Salmon, S. U., et al. (2016). Roles of forest bioproductivity, transpiration and fire in a nine-year record of cave dripwater chemistry from southwest Australia. *Geochimica et Cosmochimica Acta*, *184*, 132–150. https://doi.org/10.1016/j.gca.2016.04.017

Úbeda, X., Pereira, P., Outeiro, L., & Martin, D. A. (2009). Effects of fire temperature on the physical and chemical characteristics of the ash from two plots of cork oak (Quercus suber). *Land Degradation & Development*, *20*(6), 589–608. https://doi.org/10.1002/ldr.930

Ulery, A. L., Graham, R. C., & Amrhein, C. (1993). Wood-ash composition and soil pH following intense burning. *Soil Science*, *156*(5), 358–364. https://doi.org/10.1097/00010694-199311000-00008

Vachula, R. S., Huang, Y., Longo, W. M., Dee, S. G., Daniels, W. C., & Russell, J. M. (2019). Evidence of Ice Age humans in eastern Beringia suggests early migration to North America. *Quaternary Science Reviews*, *205*, 35–44. https://doi.org/10.1016/j.quascirev.2018.12.003

Vesper, D. J., Loop, C. M., & White, W. B. (2003). Contaminant transport in karst aquifers. *Speleogenesis and Evolution of Karst Aquifers*, *1*, 2–11.

Vilhar, U., Kermavnar, J., Kozamernik, E., Petrič, M., & Ravbar, N. (2022). The effects of large-scale forest disturbances on hydrology—An overview with special emphasis on karst aquifer systems. *Earth-Science Reviews*, *235*, 104243. https://doi.org/10.1016/j.earscirev.2022.104243

Vu, V. Q. (2011). ggbiplot: A ggplot2 based biplot [Software]. *CRAN*. Retrieved from https://cran.r-project.org/web/packages/ggbiplot/index.html

Wakeham, S. G., Schaffner, C., & Giger, W. (1980). Polycyclic aromatic hydrocarbons in recent lake sediments—I. Compounds having anthropogenic origins. *Geochimica et Cosmochimica Acta*, *44*(3), 403–413. https://doi.org/10.1016/0016-7037(80)90040-X

Wei, M., Zhang, Z., Long, T., He, G., & Wang, G. (2021). Monitoring landsat based burned area as an indicator of sustainable development goals. *Earth's Future*, *9*(6), e2020EF001960. https://doi.org/10.1029/2020EF001960

Wickham, H. (2016). ggplot2: Elegant graphics for data analysis [Software]. *CRAN*. Retrieved from https://cran.r-project.org/web/packages/ggplot2/index.html

Wickham, H. (2022). stringr: Simple, consistent wrappers for common string operations [Software]. *CRAN*. Retrieved from https://cran.r-project.org/web/packages/stringr/index.html

Wickham, H., Francois, R., Henry, L., & Muller, K. (2020). dplyr: A grammar of data manipulation [Software]. *CRAN*. Retrieved from https://cran.r-project.org/web/packages/dplyr/index.html

Wickham, H., & Henry, L. (2023). purrr: Functional programming tools [Software]. *CRAN*. Retrieved from https://cran.r-project.org/web/packages/purrr/index.html

Wickham, H., Hester, J., & Bryan, J. (2023). readr: Read rectangular text data [Software]. *CRAN*. Retrieved from https://cran.r-project.org/web/packages/readr/index.html

Wu, G., & Wang, D. Y. (2012). Mechanical and acoustic emission characteristics of limestone after high temperature. *Advanced Materials Research*, *446–449*, 23–28. https://doi.org/10.4028/www.scientific.net/AMR.446-449.23

Yang, Y., Zhang, N., Xue, M., & Tao, S. (2010). Impact of soil organic matter on the distribution of polycyclic aromatic hydrocarbons (PAHs) in soils. *Environmental Pollution*, *158*(6), 2170–2174. https://doi.org/10.1016/j.envpol.2010.02.019

Yusiharni, E., & Gilkes, R. (2012). Minerals in the ash of Australian native plants. *Geoderma*, *189–190*, 369–380. https://doi.org/10.1016/j.geoderma.2012.06.035

Zennaro, P., Kehrwald, N., Marlon, J., Ruddiman, W. F., Brücher, T., Agostinelli, C., et al. (2015). Europe on fire three thousand years ago: Arson or climate? *Geophysical Research Letters*, *42*(12), 5023–5033. https://doi.org/10.1002/2015GL064259

Zomer, R. J., Xu, J., & Trabucco, A. (2022). Version 3 of the global aridity index and potential evapotranspiration database. *Scientific Data*, *9*(1), 409. https://doi.org/10.1038/s41597-022-01493-1

References From the Supporting Information

Alshehri, T., Wang, J., Singerling, S. A., Gigault, J., Webster, J. P., Matiasek, S. J., et al. (2023). Wildland-urban interface fire ashes as a major source of incidental nanomaterials. *Journal of Hazardous Materials*, *443*, 130311. https://doi.org/10.1016/j.jhazmat.2022.130311

Johansen, M. P., Hakonson, T. E., Whicker, F. W., & Breshears, D. D. (2003). Pulsed redistribution of a contaminant following forest fire: Cesium-137 in runoff. *Journal of Environmental Quality*, *32*(6), 2150–2157. https://doi.org/10.2134/jeq2003.2150a

Ku, P., Tsui, M. T.-K., Nie, X., Chen, H., Hoang, T. C., Blum, J. D., et al. (2018). Origin, reactivity, and bioavailability of mercury in wildfire ash. *Environmental Science & Technology*, *52*(24), 14149–14157. https://doi.org/10.1021/acs.est.8b03729

Pebesma, E., & Bivand, R. (2023). *Spatial data science: With applications in R* (1st ed.). Chapman and Hall/CRC. https://doi.org/10.1201/9780429459016